



State of the art and perspectives of CMOS avalanche detectors

Lucio Pancheri

DII, University of Trento & TIFPA-INFN, Italy

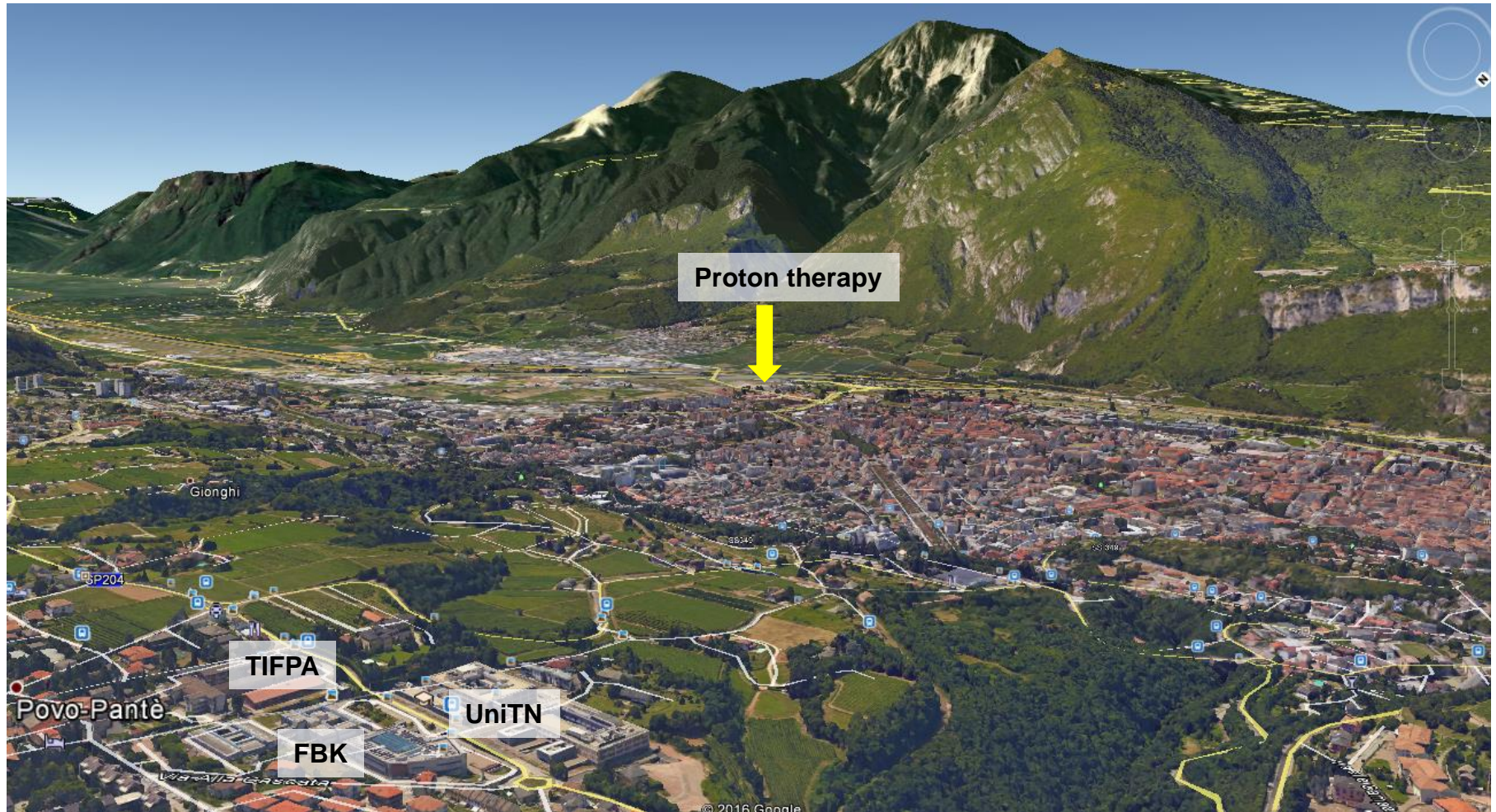
CERN seminar

January 20, 2017



Research on silicon detectors in Trento







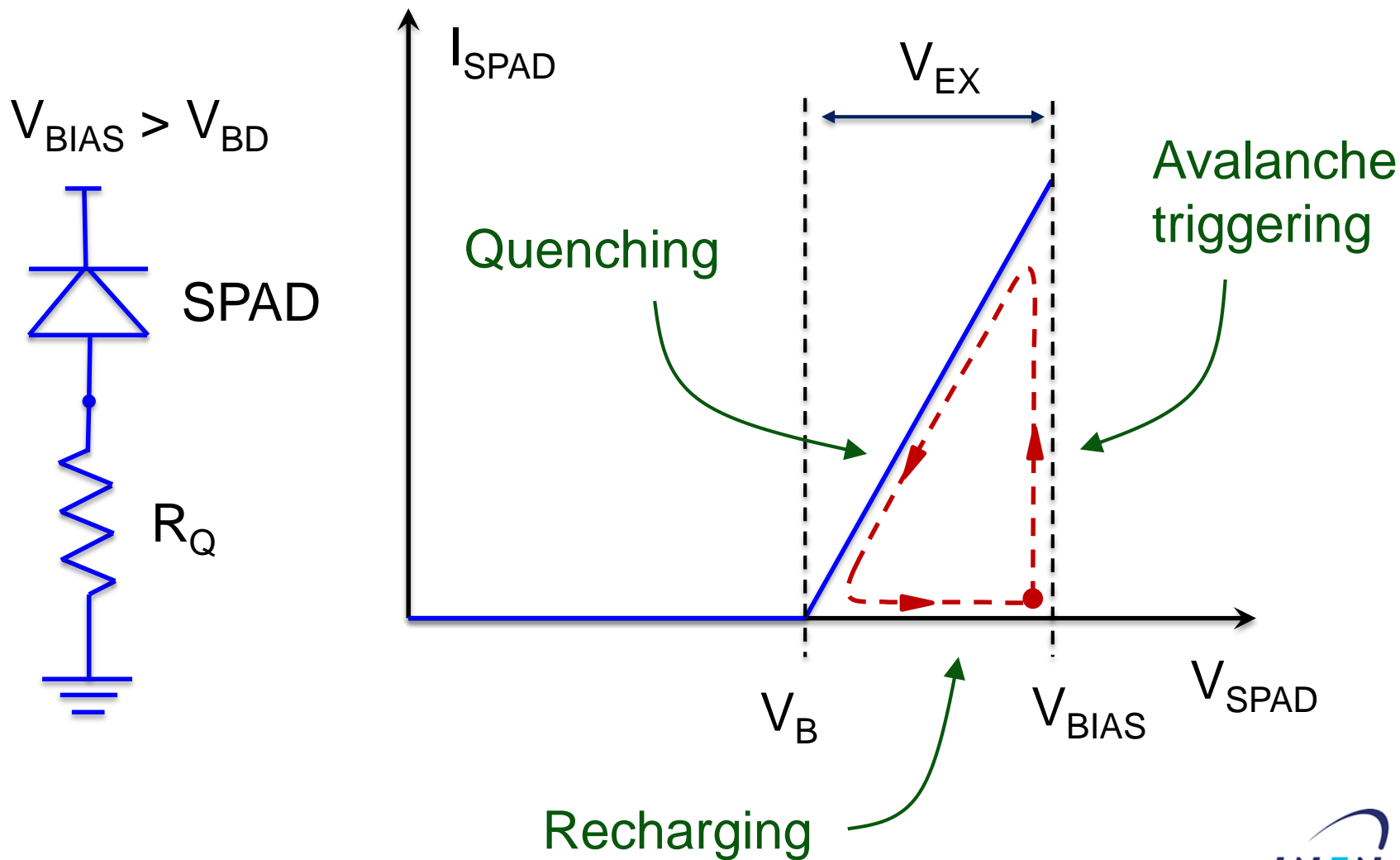
Outline

- Introduction
- CMOS-integrated single-photon detectors: an overview
- APiX: Geiger-mode avalanche pixel detectors for ionizing particles
- Conclusion and future perspectives



Geiger-mode avalanche detectors

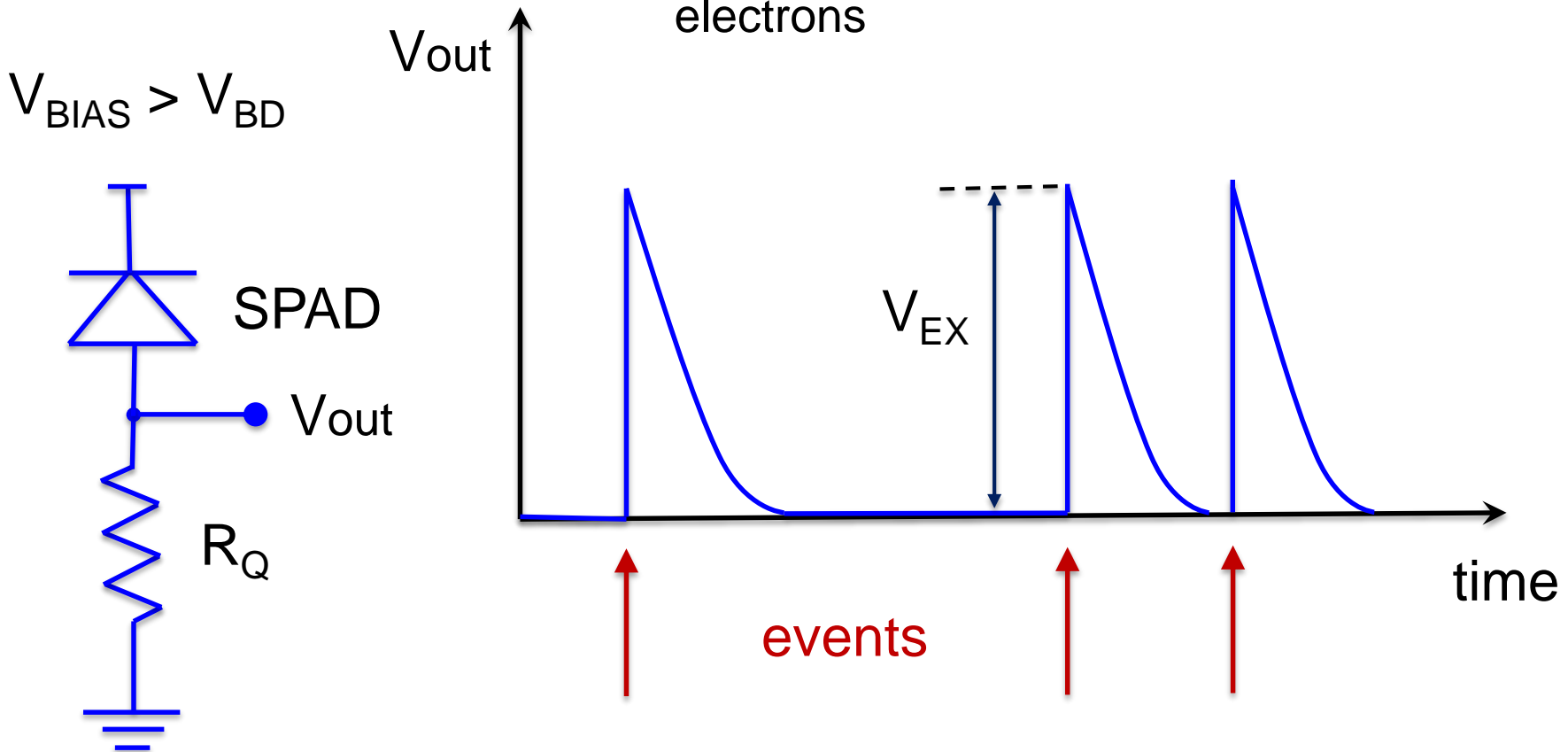
a.k.a. Single-Photon Avalanche Diodes (SPADs), SiPM cell





Geiger-mode avalanche detectors

1 primary generated electron-hole pair:
very large current pulse $\sim 10^5 - 10^6$
electrons





CMOS SPAD characteristics

Features:

- Single-photon sensitivity → shot noise limited
- Excellent timing resolution: ~ 100 ps FWHM

CMOS:

Monolithic integration of SPAD and processing electronics

Arrays → **single-photon imaging**

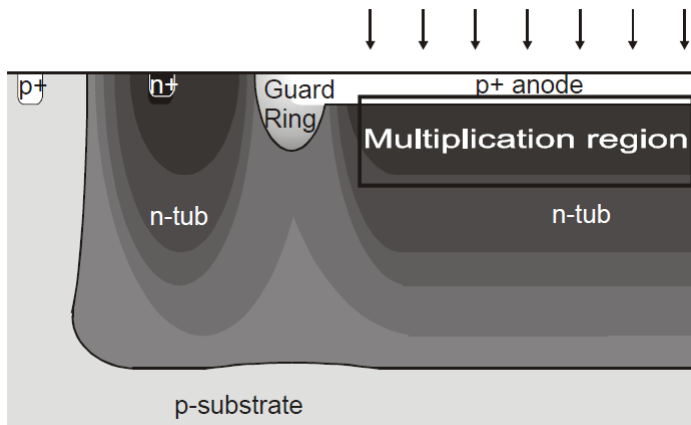


Outline

- Introduction
- CMOS-integrated single-photon detectors: an overview
- APiX: Geiger-mode avalanche pixel detectors for ionizing particles
- Conclusion and future perspectives



CMOS SPADs: early example at EPFL



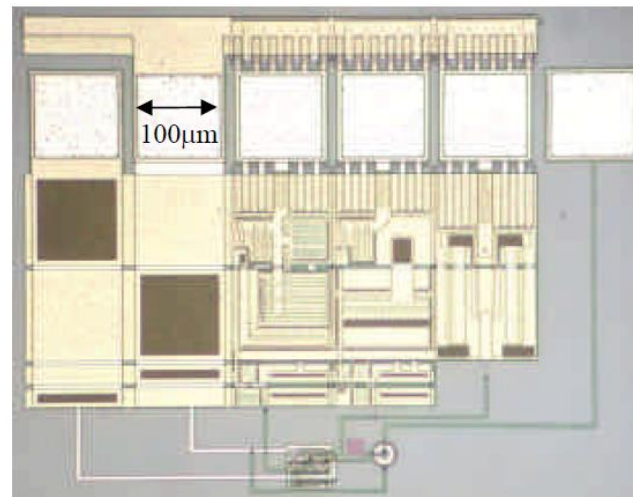
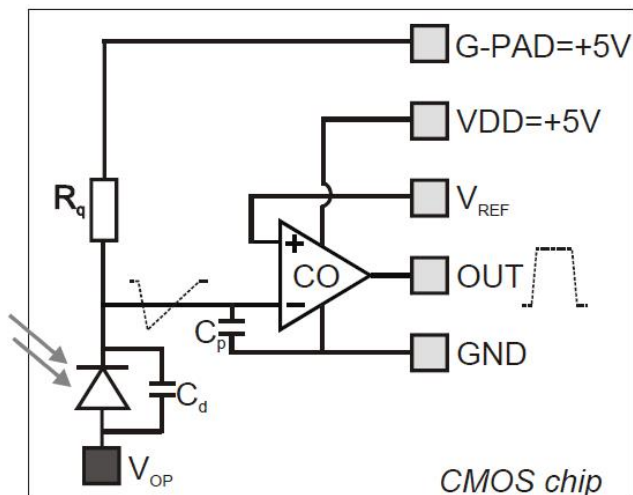
Process: **CMOS 0.8 μm**

Area: $30\mu\text{m}^2$

Peak PDE: 20%

DCR: 300 Hz

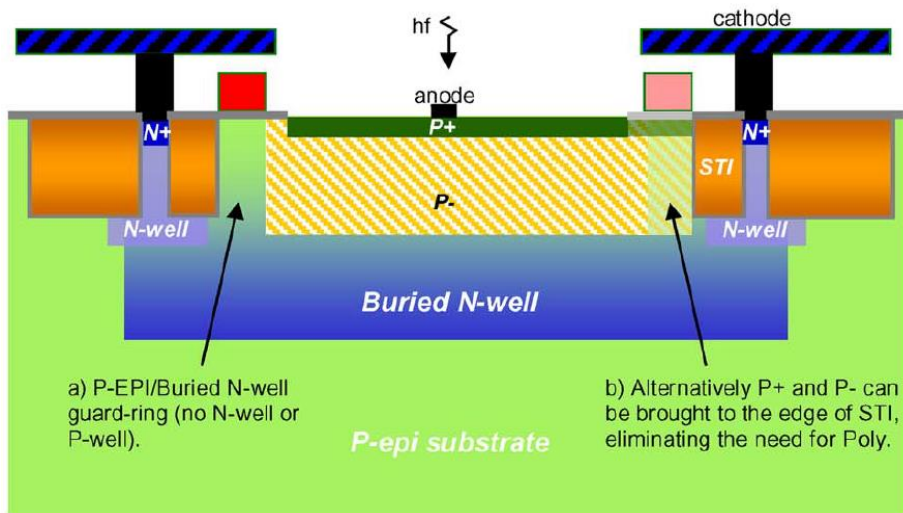
Timing resolution: 50 ps FWHM



A. Rochas et al., Proc. SPIE 2003



CMOS SPADs: deep submicron



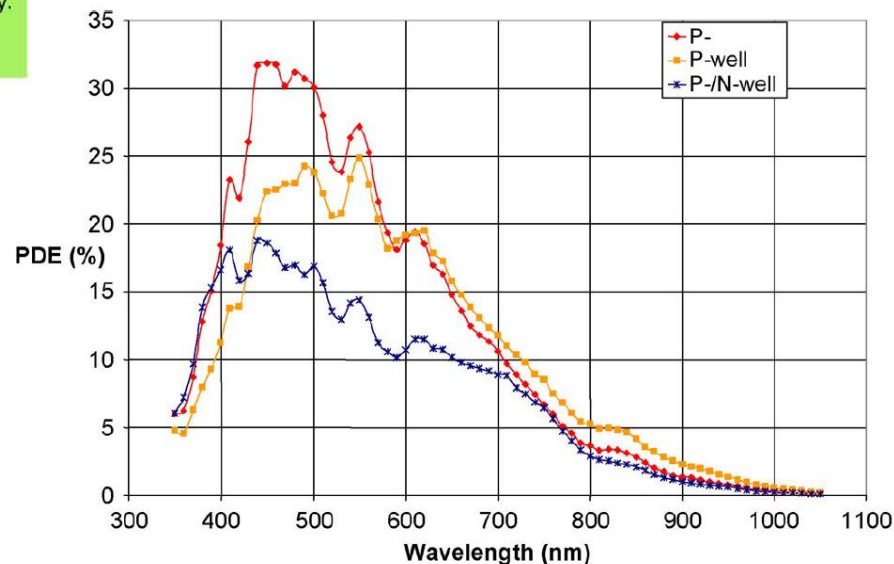
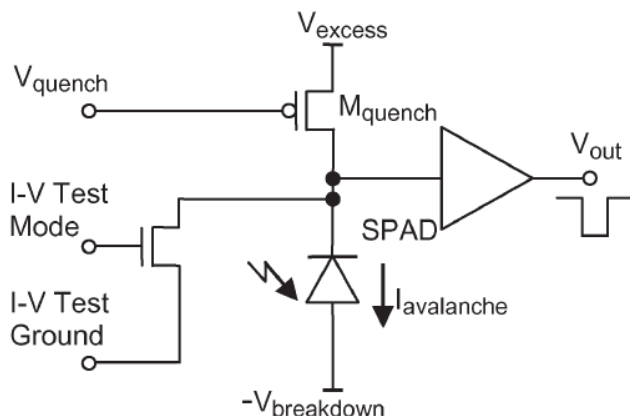
Process: **CMOS 130 nm**

Area: $50\mu\text{m}^2$

Peak PDE: 33%

DCR: 40 Hz

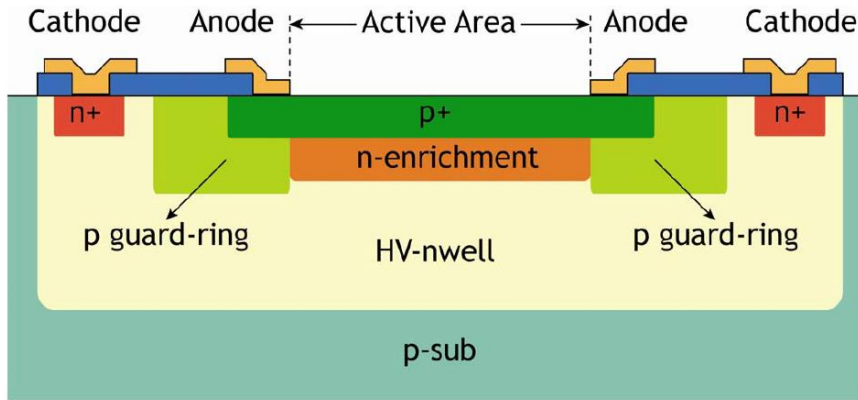
Timing resolution: 237 ps FWHM



J. Richardson et al., IEEE Trans. Electron Dev. **2011**



CMOS SPADs: high efficiency



Process: **CMOS 350nm**

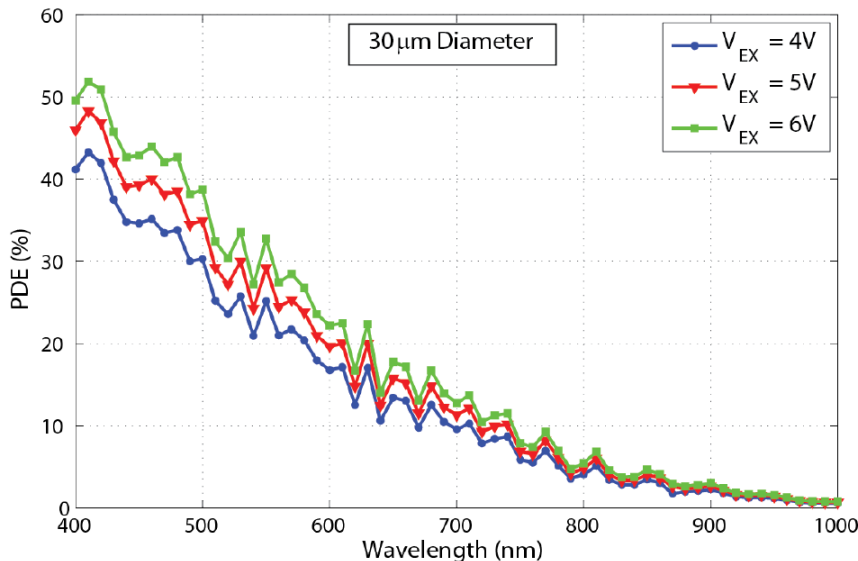
**Imaging with custom
implantation**

Area: $700\mu\text{m}^2$

Peak PDE: > 50%

DCR: 50 Hz

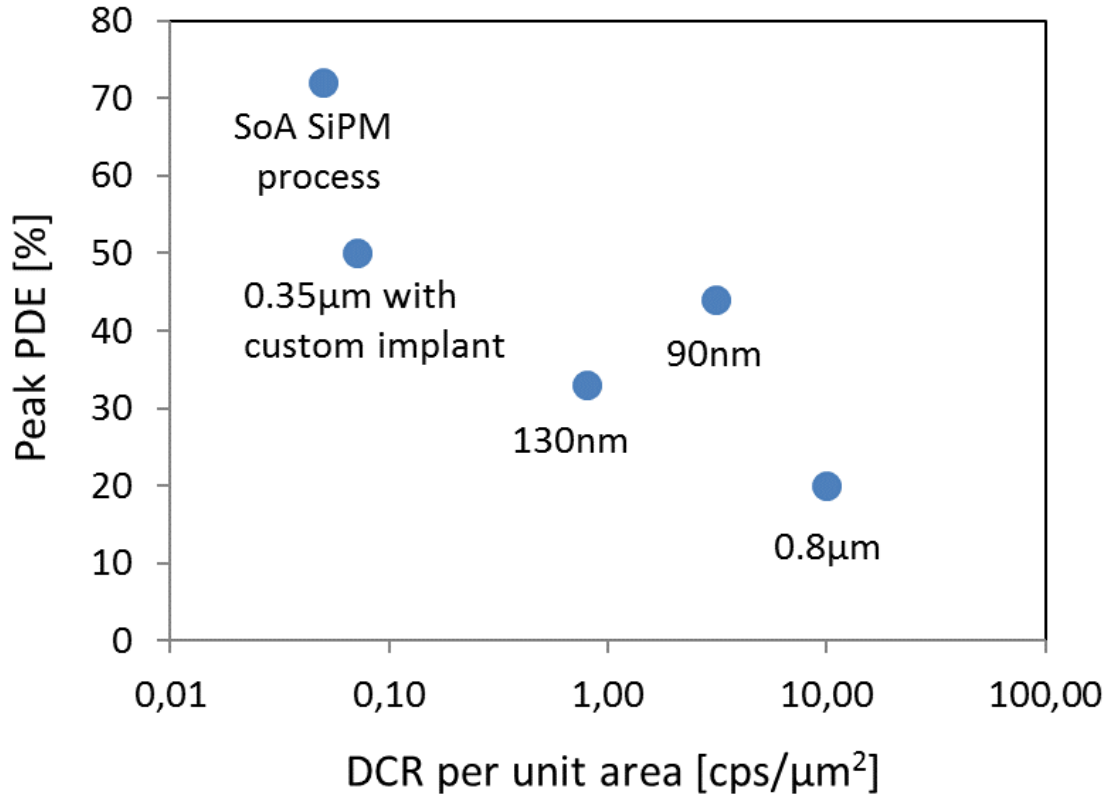
Timing resolution: 142 ps FWHM



D. Bronzi et al., Proc. IEEE ESSDERC 2012



Summary and comparison with SiPM



SiPM:

For major manufacturers
PDE > 70% (single cell, not
considering FF)

DCR ~ 50 kHz/mm²

With customization, CMOS can approach SiPM performance

For a complete overview, see D. Bronzi, et al., IEEE Sensors J. 2016



SPAD array applications

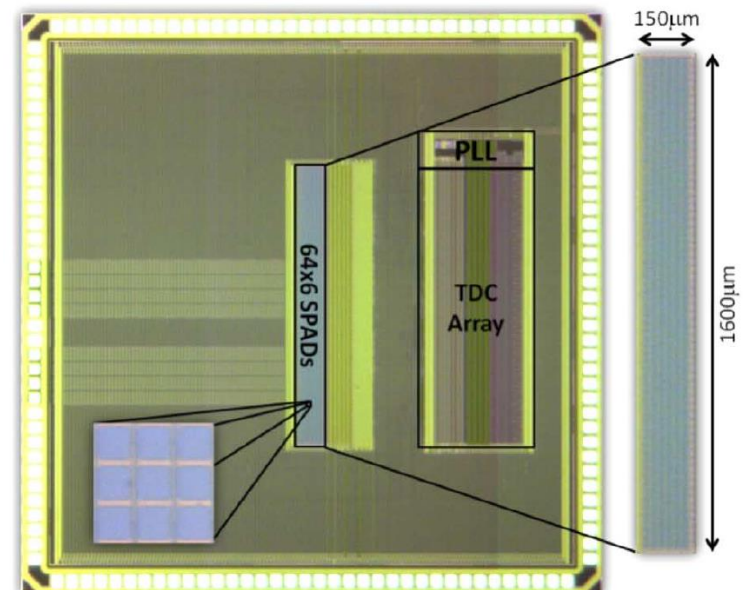
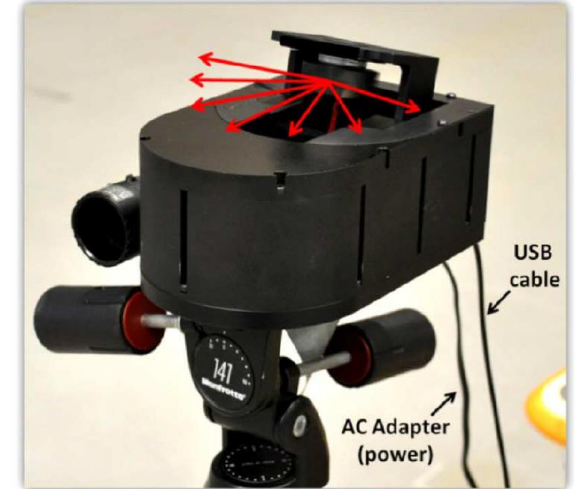
- Time-Of-Flight optical ranging, LIDAR
- Fluorescence spectroscopy
- Raman spectroscopy
- Gamma ray detection (PET)
- Quantum cryptography
- ...



Time-of-Flight optical ranging

Automotive LIDAR developed by Toyota

- 180nm CMOS
- SPAD array with integrated TDCs
- 70% array Fill Factor
- Distance range: 100 m



C. Niclass et al., IEEE J. Solid-State Circuits, 2013

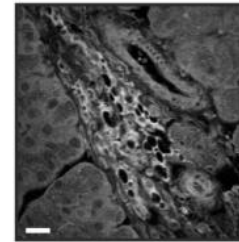


Fluorescence microscopy

Multi-parametric fluorescence imaging

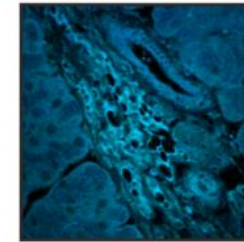
- 350nm CMOS (AMS)
- 4-line SPAD array
- Sub-ns gated counters
- 36% Fill Factor

Intensity



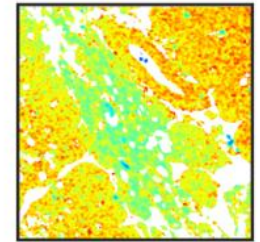
0 1,000
photons

Color

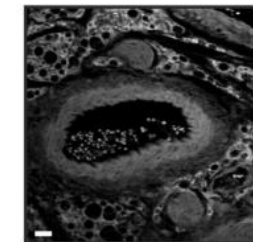


ex: 840nm

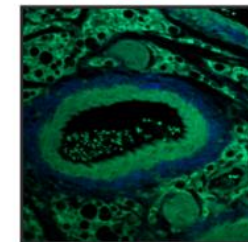
Lifetime



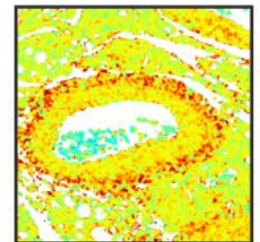
0.5 2.5
lifetime (ns)



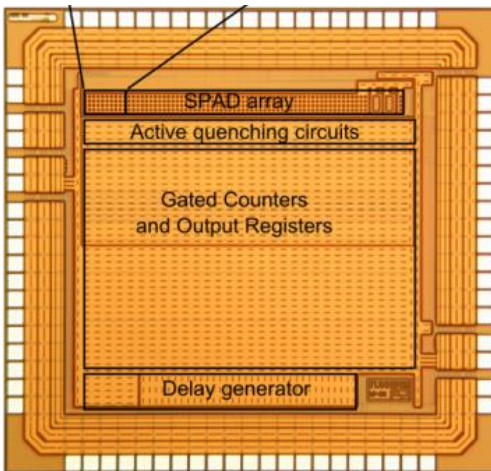
0 1,250
photons



ex: 920nm



0.5 3.5
lifetime (ns)



Label-free imaging of unstained liver tissue excised from a tumorigenic murine model

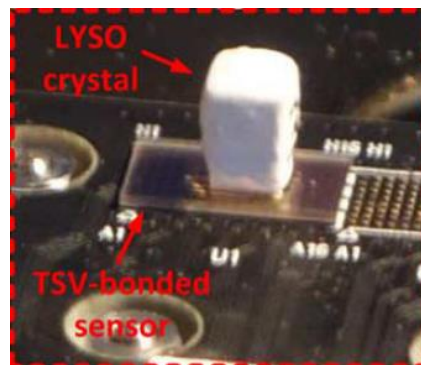
M. Popleteeva et al., Opt. Expr, 2015



Digital SiPMs for PET

SPADNET project (EU FP7)

- 130nm CMOS process
- Large pixels including 180 SPADs (Mini-SiPM)
- integrated TDCs
- 42.6 % pixel Fill Factor

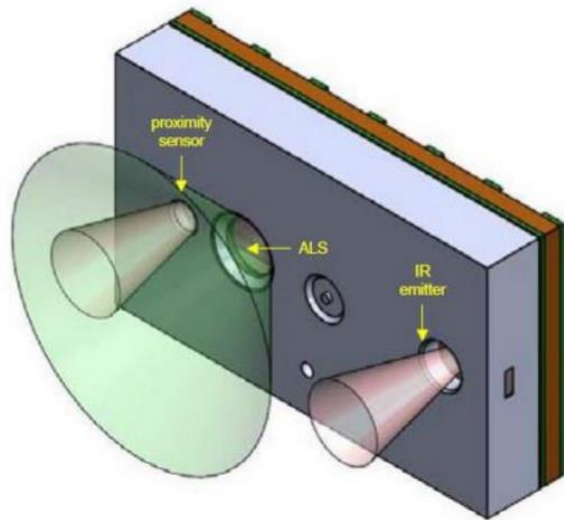
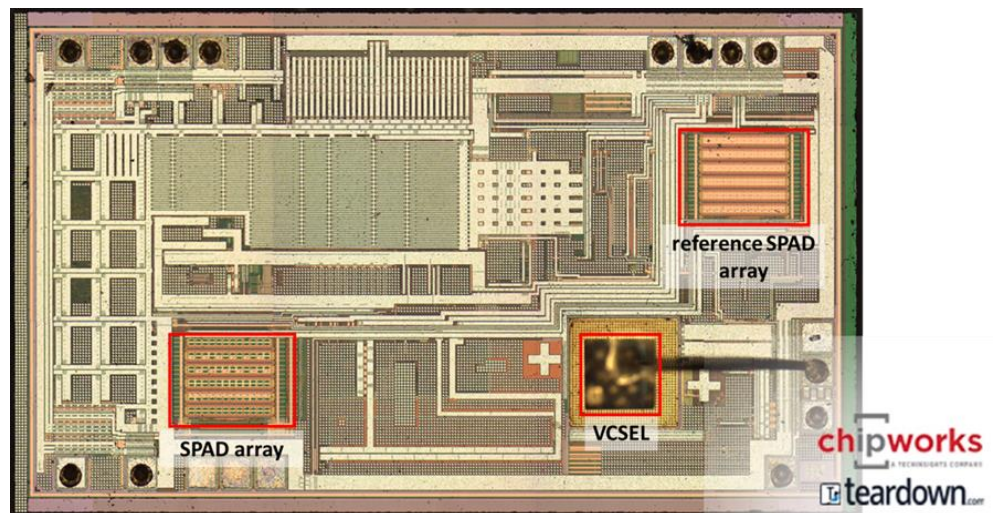
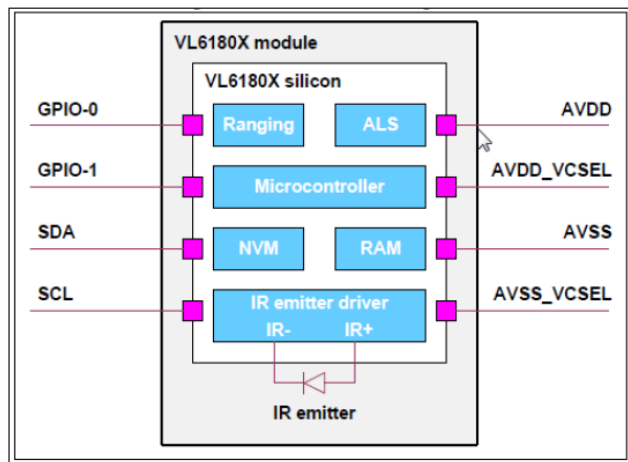


L. Braga et al., IEEE J. Solid-State Circuits, 2014



First consumer products: ST ToF sensor

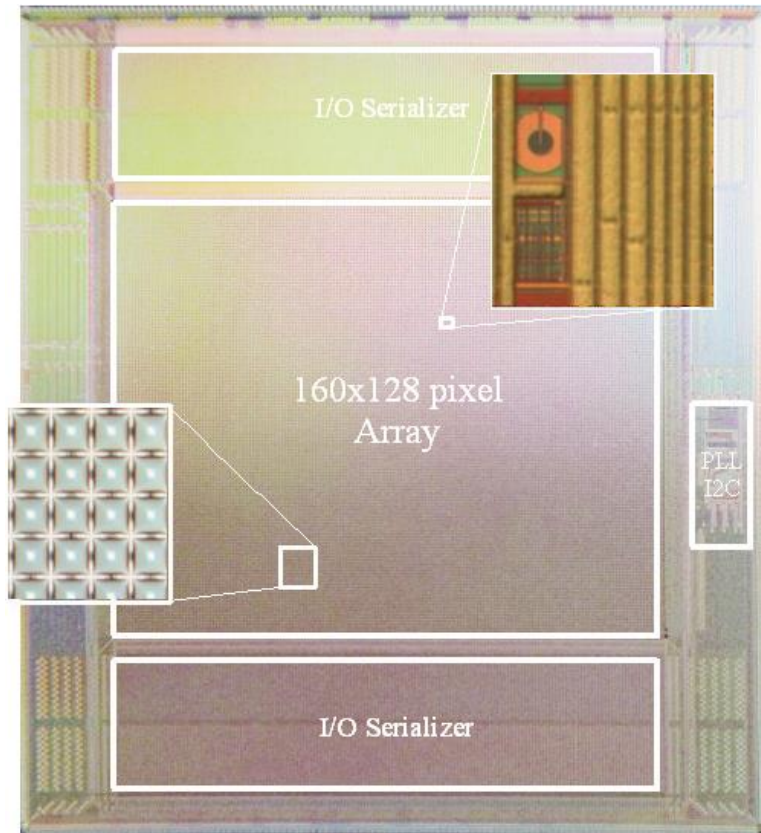
Proximity sensor based on SPAD array and pulsed VCSEL



- Presented in **2014**
- Mobile applications (mounted on iPhone7)
- Low power
- Short range (15 cm)



SPAD image sensor



C. Veerappan et al., ISSCC 2011

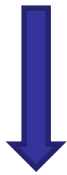
MegaFrame EU project (FP6)

- 160 x 128 pixel array
- Technology: 130nm CMOS
- In-pixel Time-to-Digital Conv.
- 140ps timing resolution
- **Pixel pitch: 50um**
- **Fill factor: 1%**



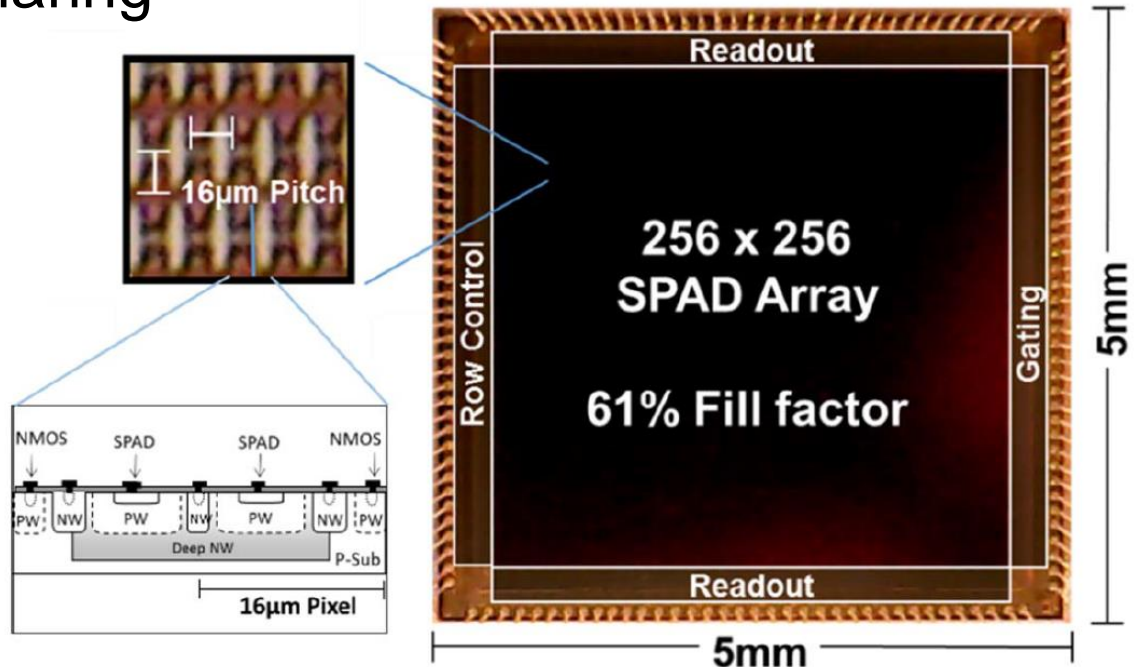
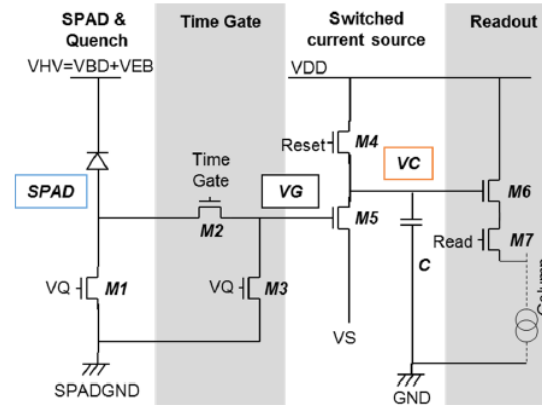
Improving the Fill Factor

- 16 μm x 16 μm pixel
- 65nm CMOS
- binary pixel (7 transistors)
- SPAD deep nwell sharing
- Improved SPAD GR



61% Fill Factor

I. Gyongy et al., IEDM 2016

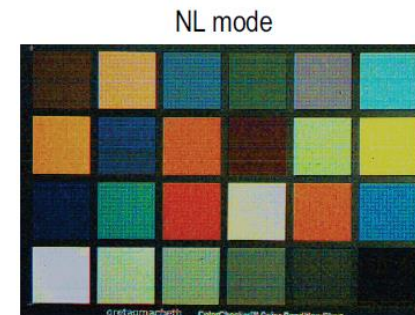
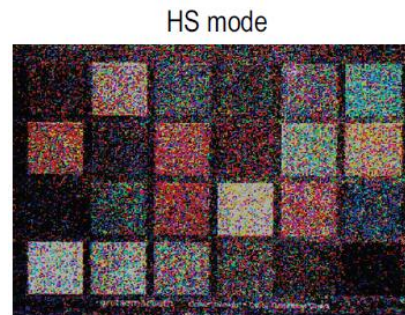
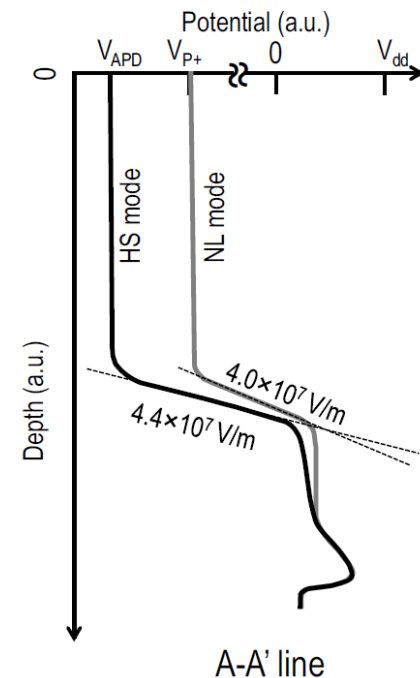
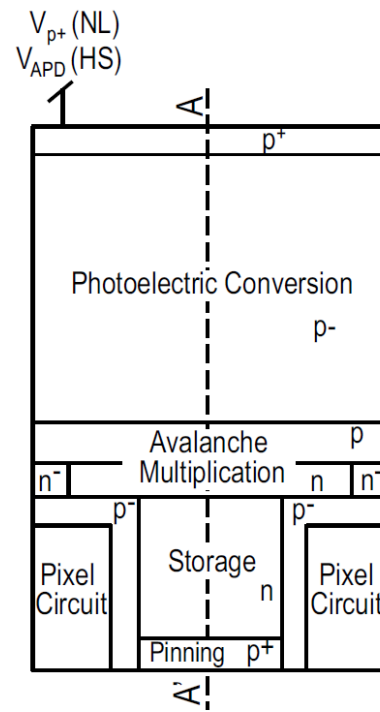




Deep APD

Panasonic project

- 110nm CMOS
- Backside illumination
- **Avalanche multiplication region below electronics**
- Pixel pitch $3.8\mu\text{m}$
- 4 transistors / pixel
- Linear and binary mode

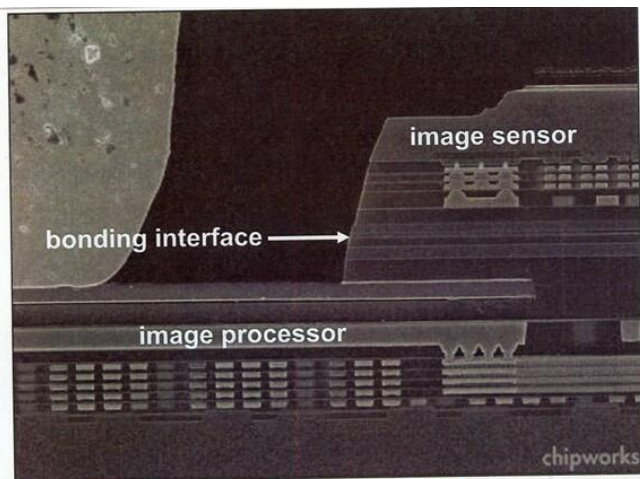


M. Mori et al., ISSCC 2016

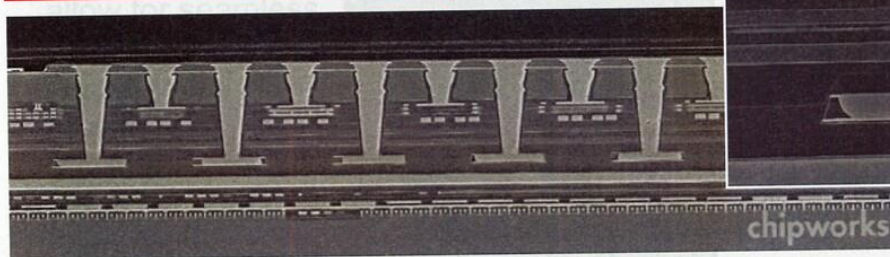


3D integration

High density interconnections successfully demonstrated for image sensors

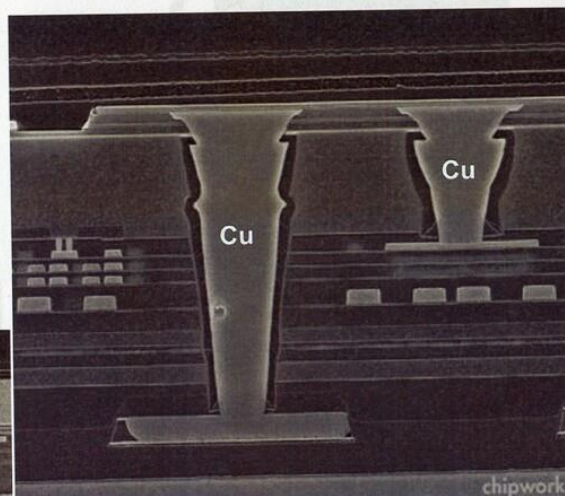


SEM cross-section of stacked dies



SEM cross-section of TSVs

Sony 13 Mpixel stacked image sensor (2013)



electroiq.com



3D-integrated SPAD image sensor 1

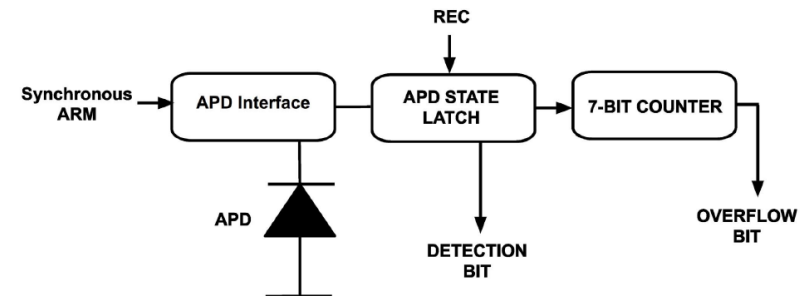
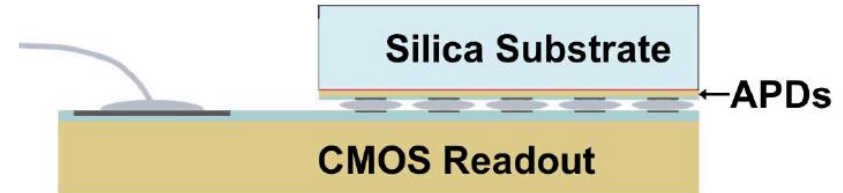
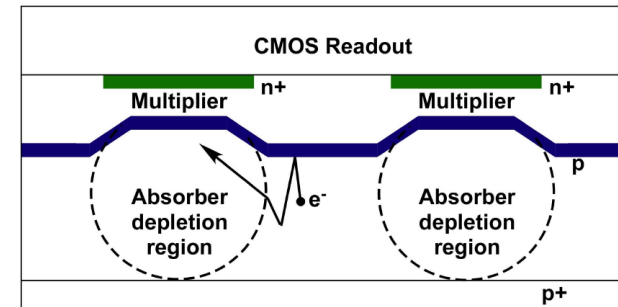
MIT Lincoln Laboratory

- 25 μm pitch
- 180nm CMOS + custom (APDs)
- 7-bit counter/pixel
- Backside illumination



10 - 20% detection efficiency
(limited by optical cross-talk)

B. Aull et al., IEEE Sensors J., 2015





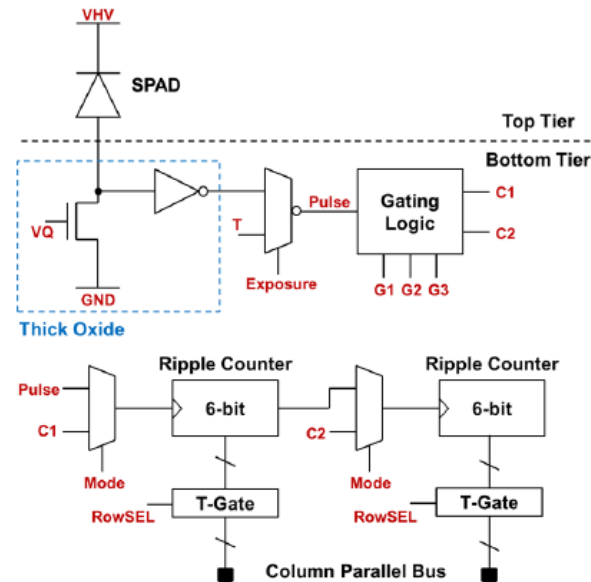
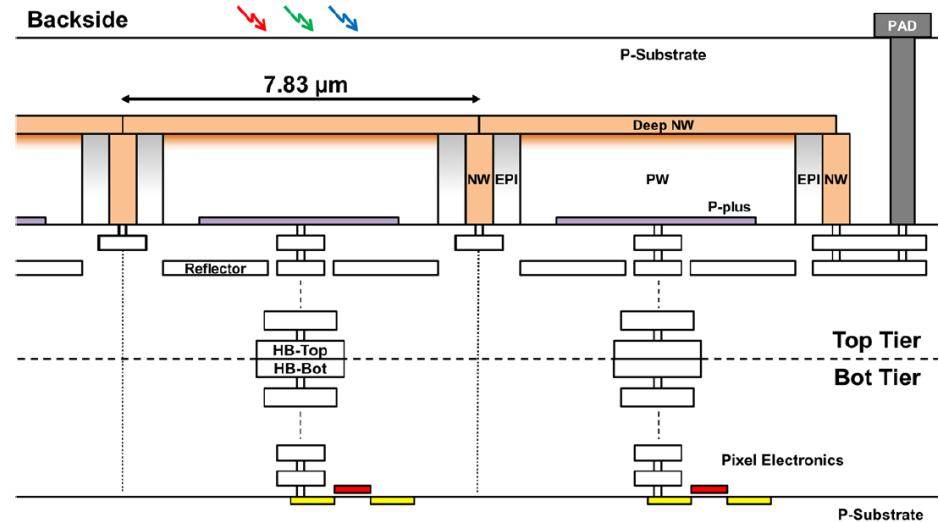
3D-integrated SPAD image sensor 2

- 7.83 μm pitch
- 65nm CMOS (top) + 40nm CMOS (bottom)
- 2 6-bit counters/pixel
- Backside illumination



45% Fill Factor

T. Al Abbas et al., IEDM 2016



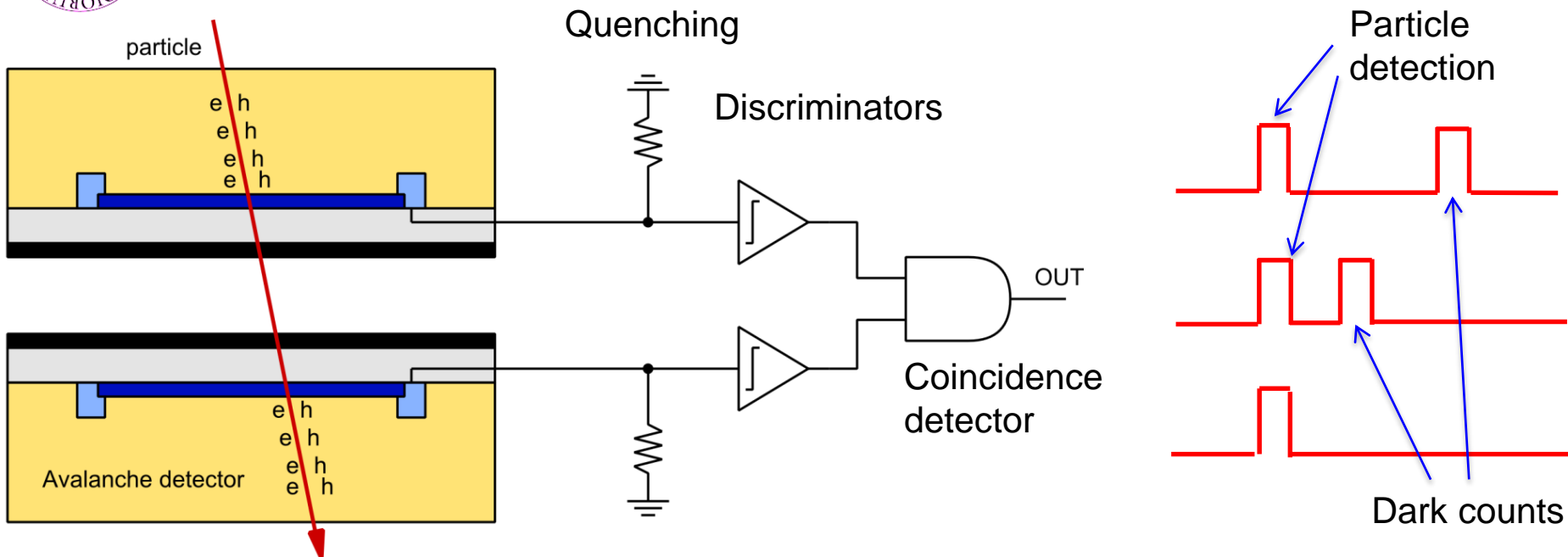


Outline

- Introduction
- CMOS-integrated single-photon detectors: an overview
- **APiX: Geiger-mode avalanche pixel detectors for ionizing particles**
- Conclusion and future perspectives



APIX particle detector concept



- Two Geiger-mode avalanche detectors in **coincidence**:

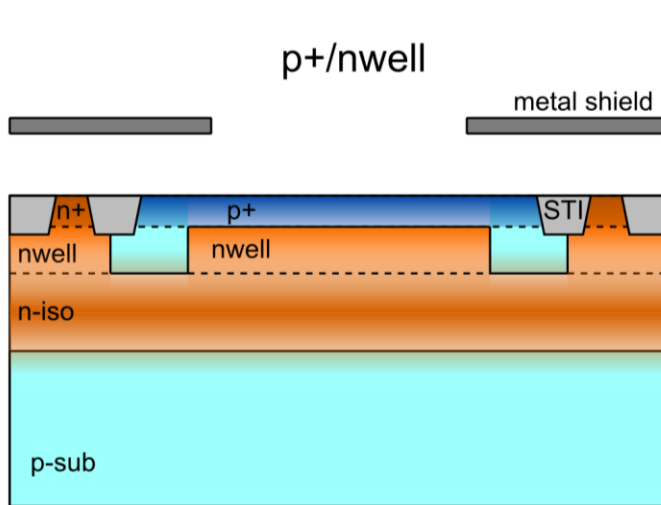
$$DCR = DCR_1 \times DCR_2 \times 2\Delta T$$

- In-pixel coincidence: integrated electronics is needed:
CMOS avalanche detectors



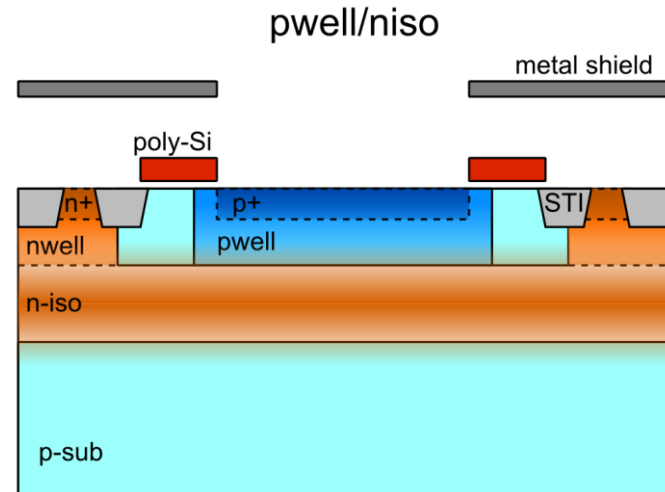
SPADs in 150nm CMOS process

- **Standard CMOS** process – no modifications
- Avalanche diodes in deep nwell: **isolated from substrate**



Type 1:

- Shallow step junction
- Active thickness ~ 1 μm



Type 2:

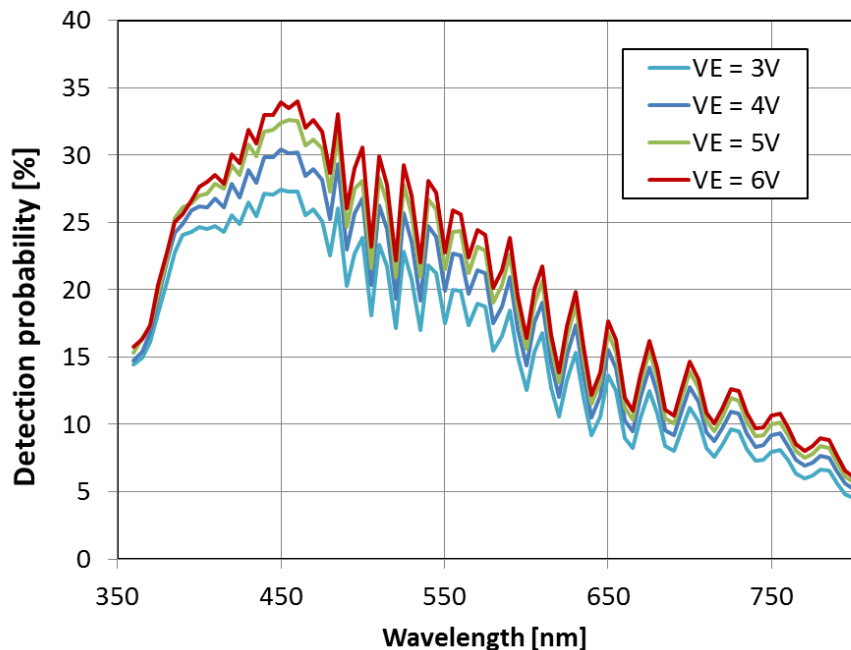
- Deep graded junction
- Active thickness ~ 1.5 μm

L. Pancheri, D. Stoppa, ESSDERC 2011



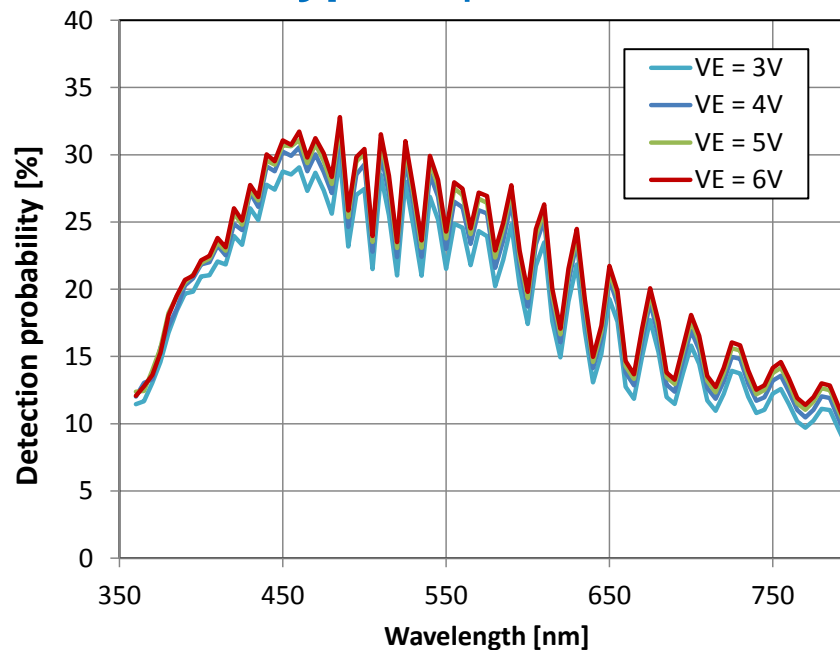
Photo-Detection Efficiency

Type 1: p+/nwell



Shallower junction:
better NUV – Blue efficiency

Type 2: pwell/niso



Wider depletion region:
Better red-IR efficiency

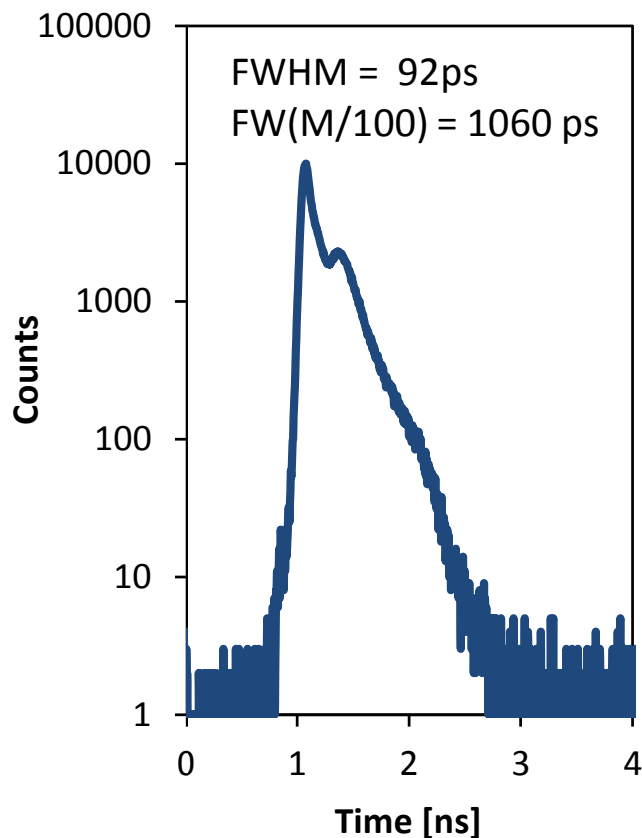
L. Pancheri et al., J. Selected Topics in Quantum Electron, 2015



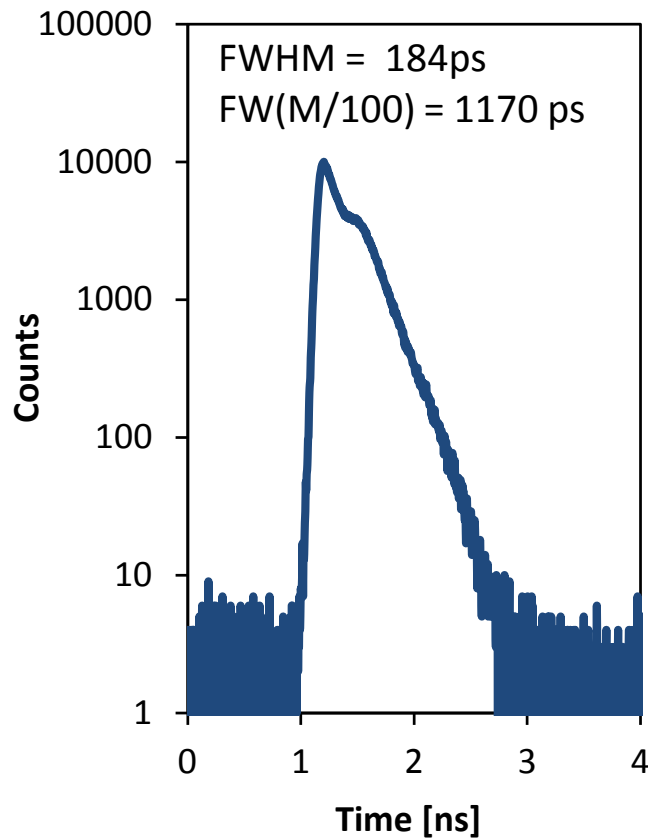
Single-photon timing resolution

Measured on 10- μm devices, with blue laser (470nm), 70ps FWHM

Type 1: 60ps FWHM

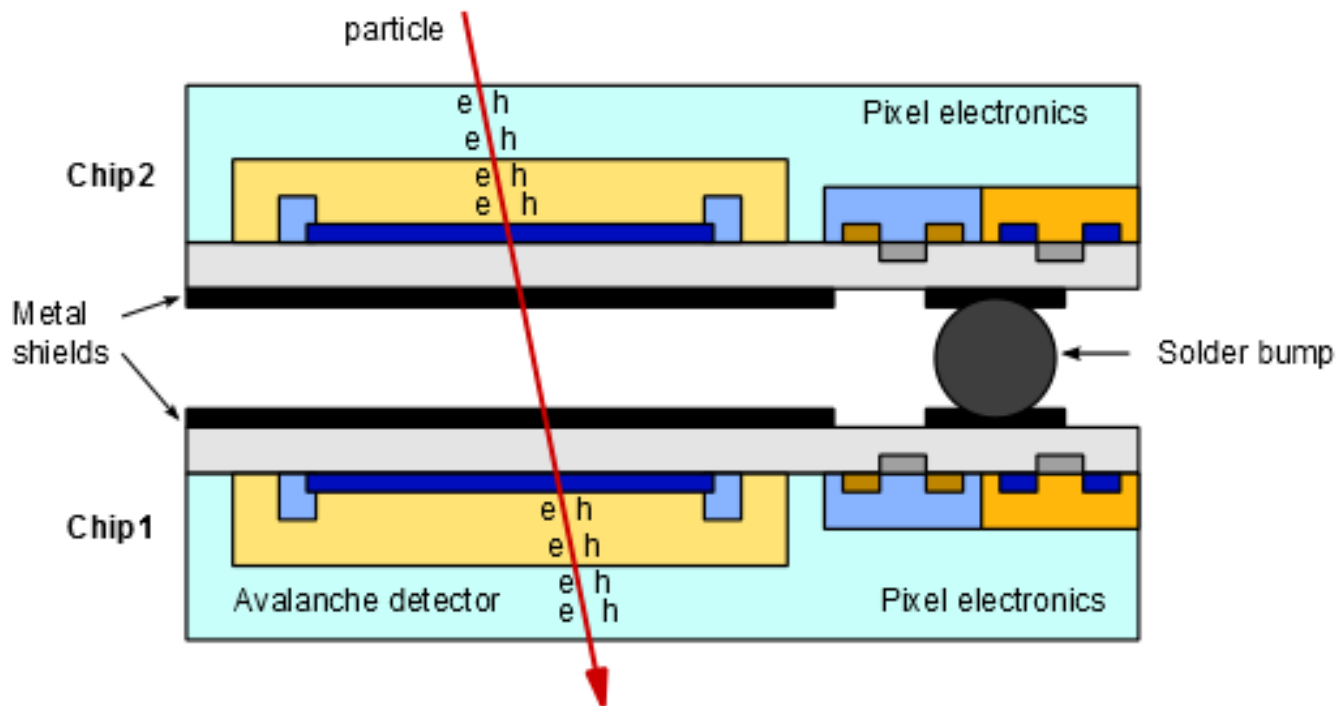


Type 2: 170ps FWHM





Proof-of-concept demonstrator



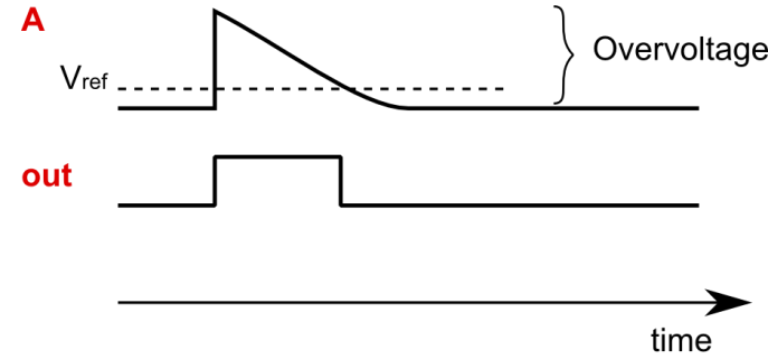
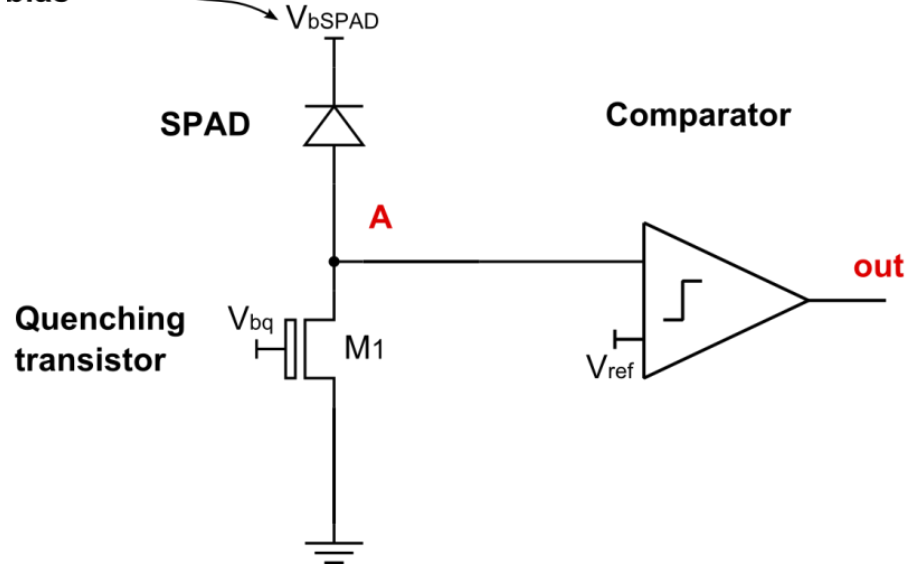
2-layer pixel cross section:

- Electronic readout on both layers
- **Metal shielding** from optical cross-talk
- Vertical interconnection by **bump bonding**



Pixel architecture

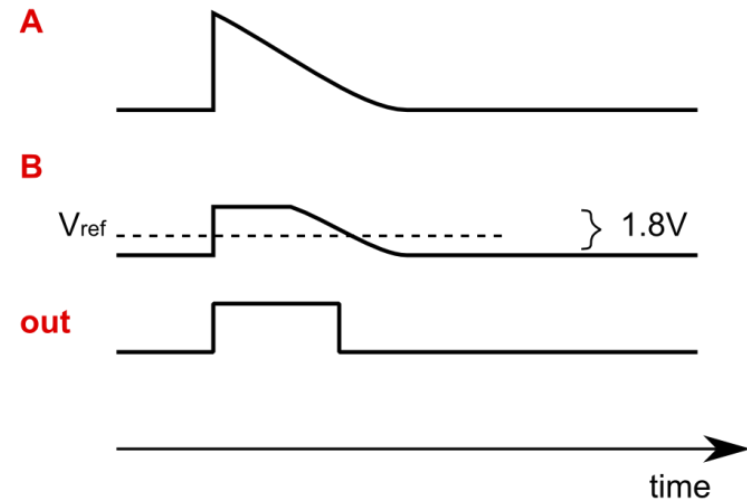
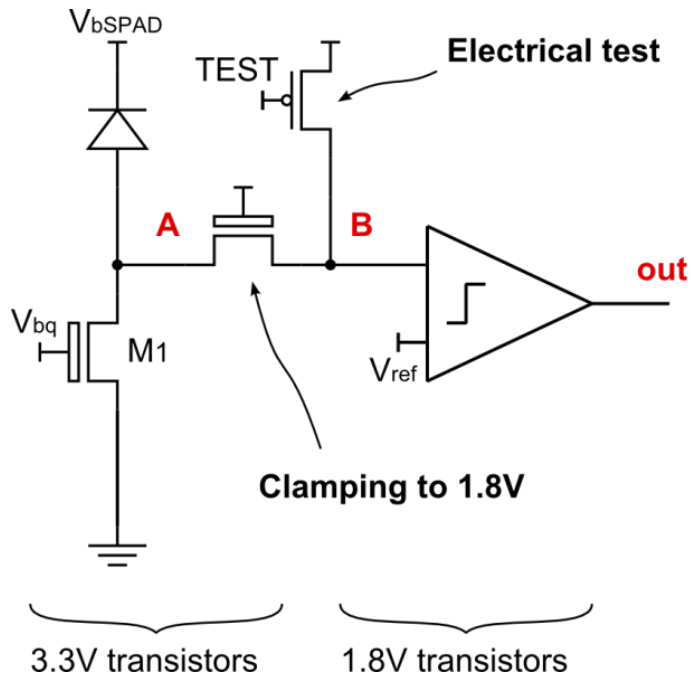
High Voltage bias



- **High voltage** V_{bSPAD} applied at nwell
- Maximum voltage at node A: $V_{ov} = V_{bSPAD} - V_{BD}$
- **Small capacitance** at node A
- Passive quenching with constant current recharge



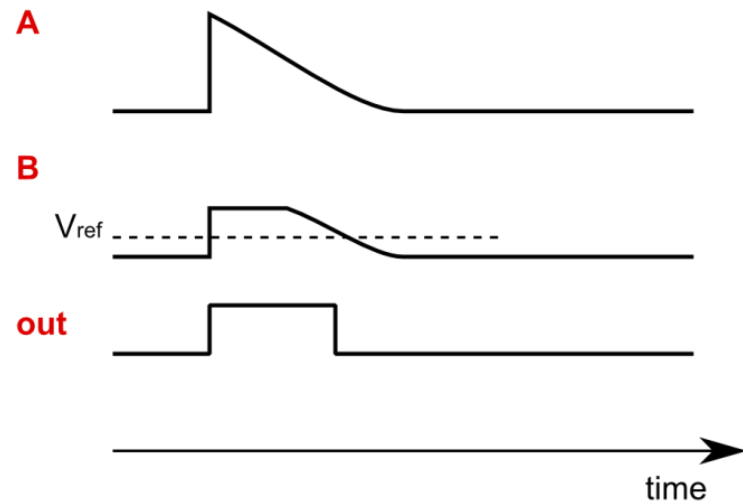
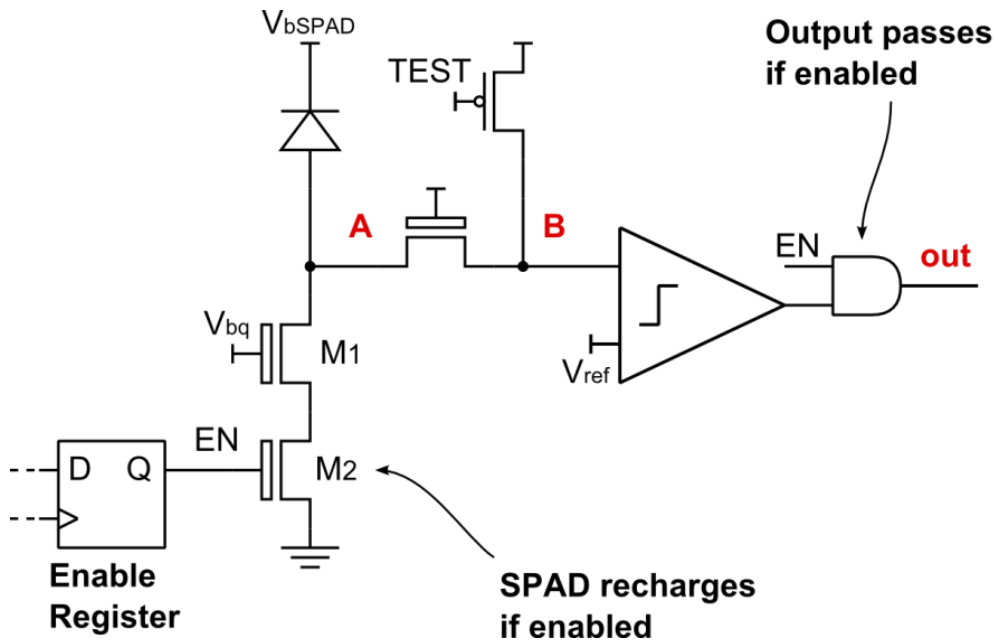
Pixel architecture



- Front-end transistors: 3.3V → Maximum overvoltage 3.3V
- **Digital circuitry: 1.8V** compact – fast – low-power



Pixel architecture: enable register

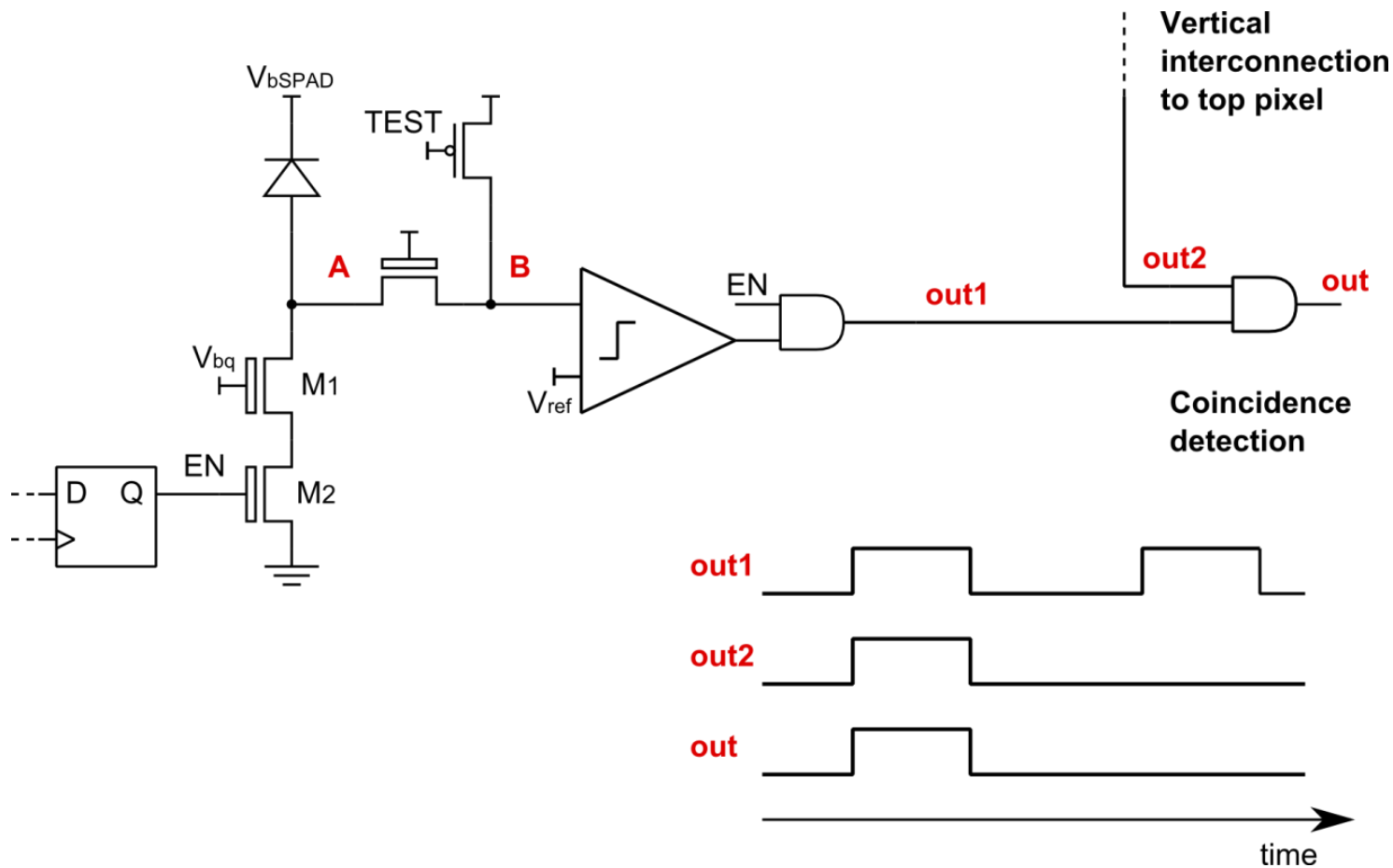


Pixels can be **individually disabled**:

- M_2 disables recharge
- Output and gate blocks output pulses



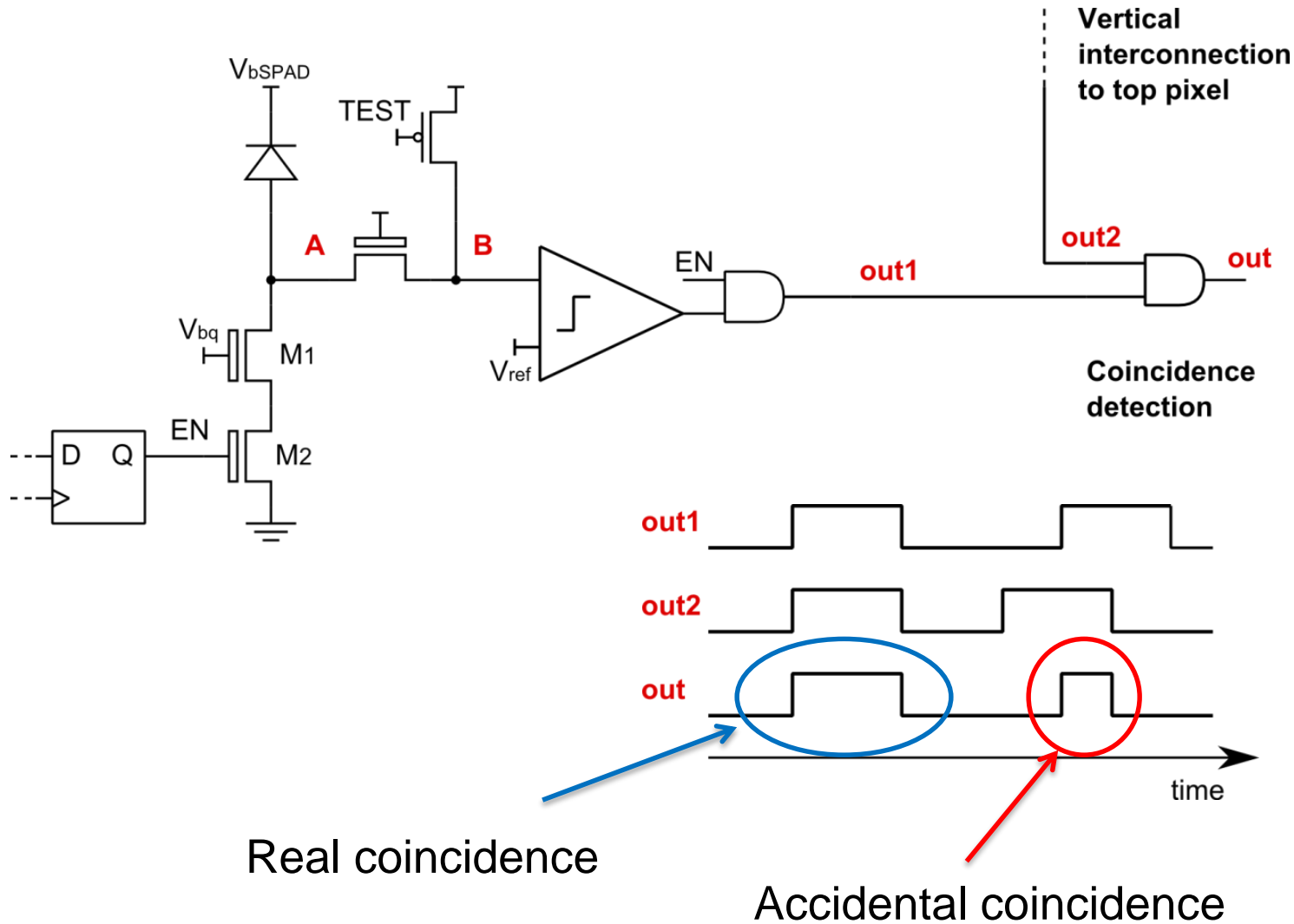
Pixel architecture: coincidence



- Coincidence with top-layer pixel

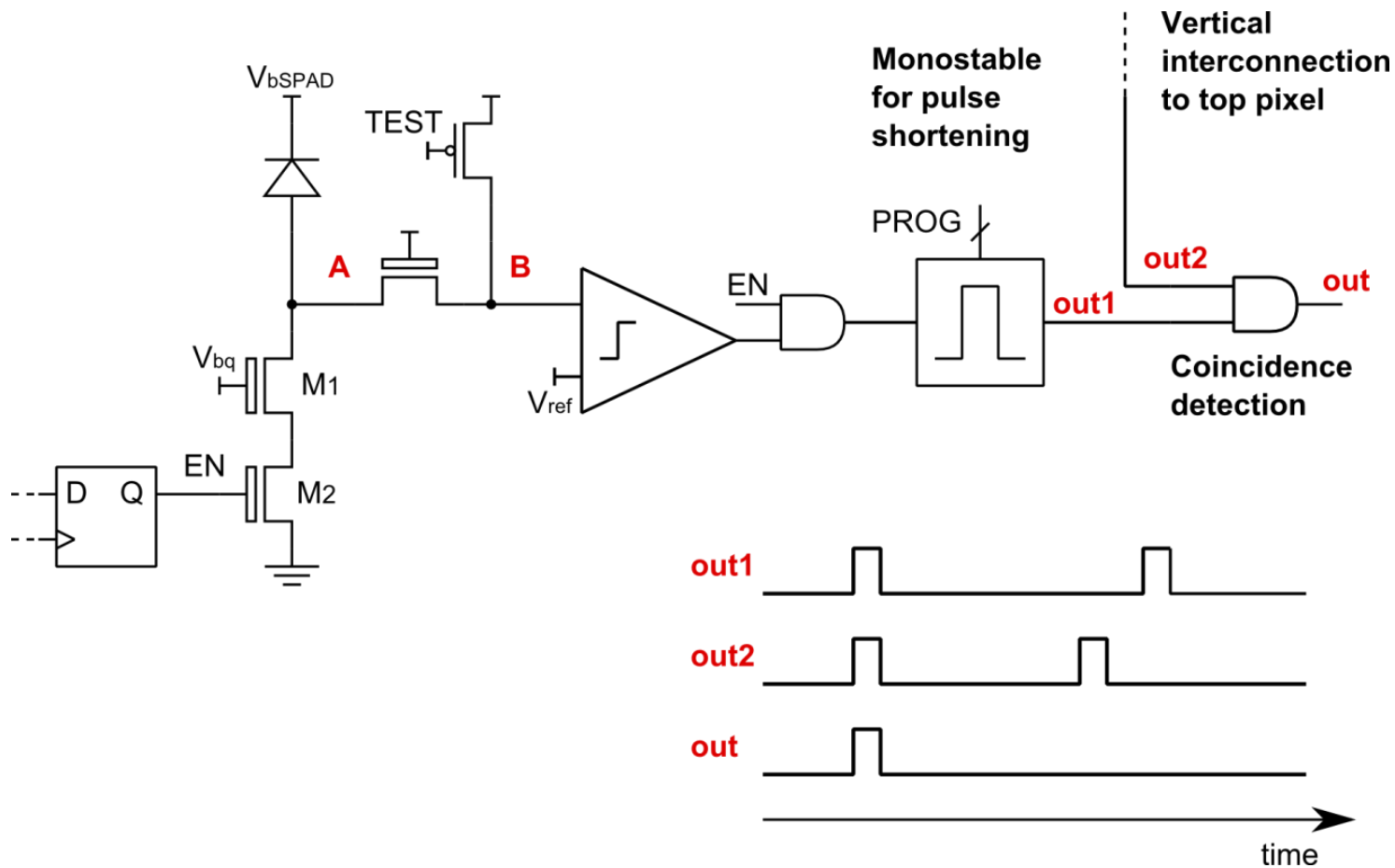


Pixel architecture: coincidence





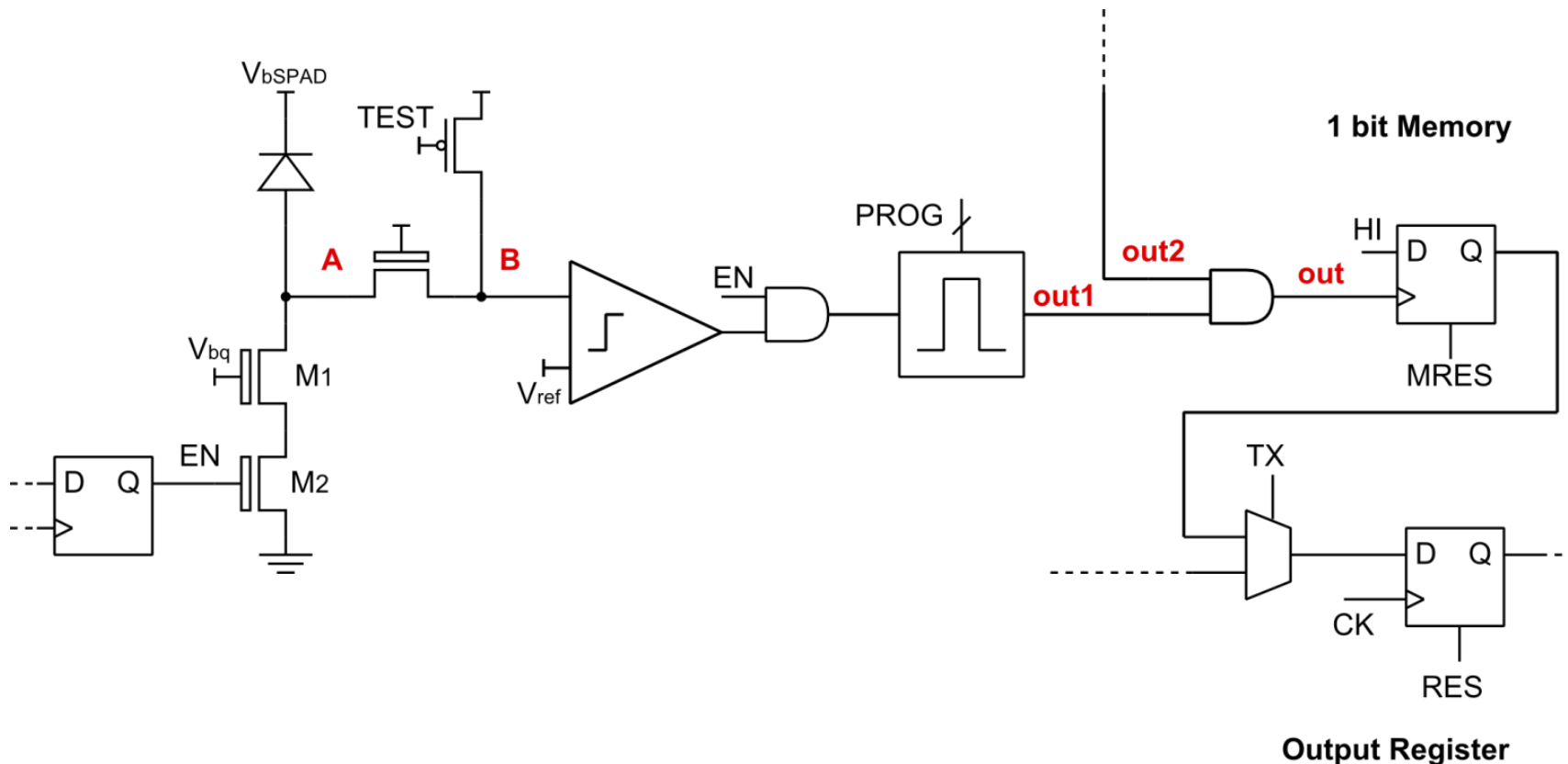
Pixel architecture: monostable



- Pulse shortening: reduces the rate of accidental coincidence
- Programmable pulse width: **750ps, 1.5ns, 10ns**



Pixel architecture: storage

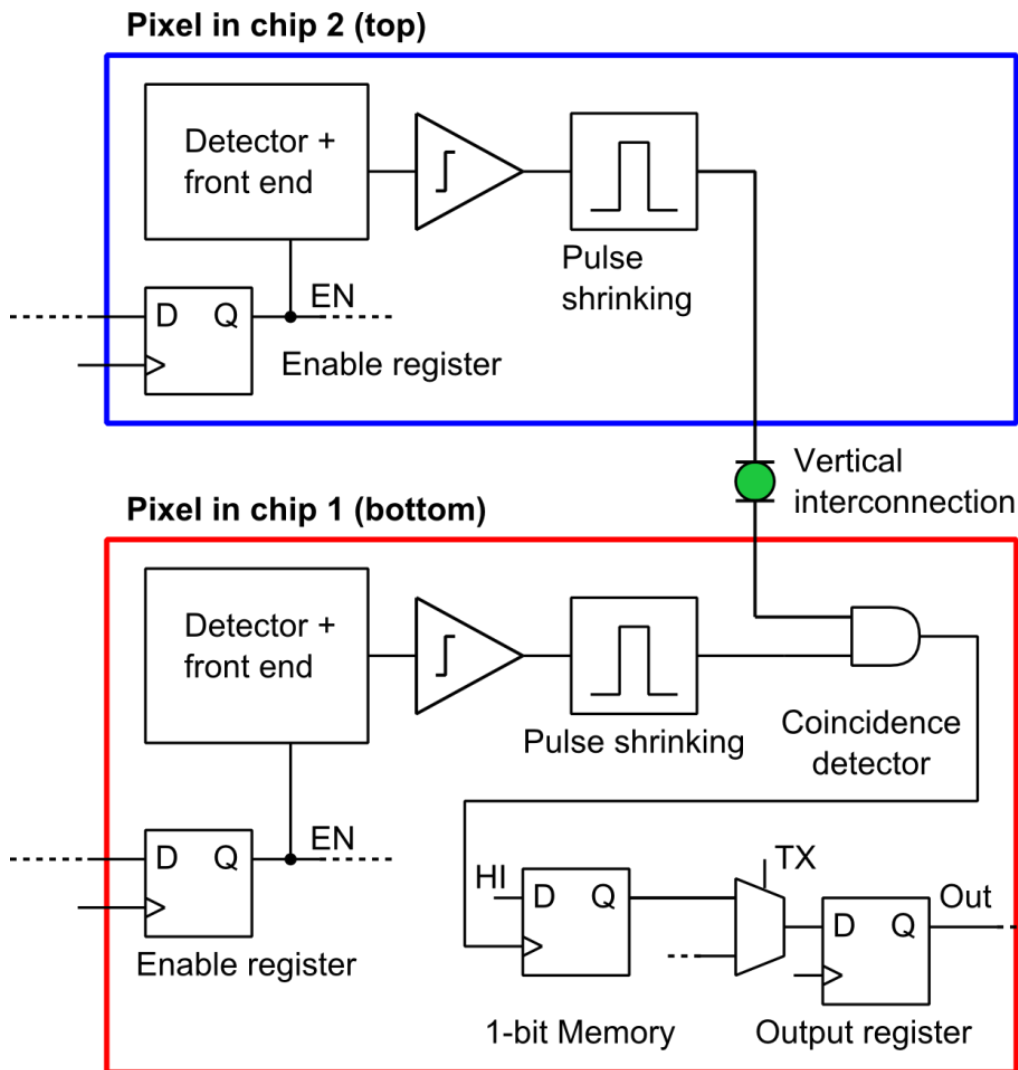


- **Global shutter** operation:
 - Fast transfer from memory to output register
 - Simultaneous accumulation and data output



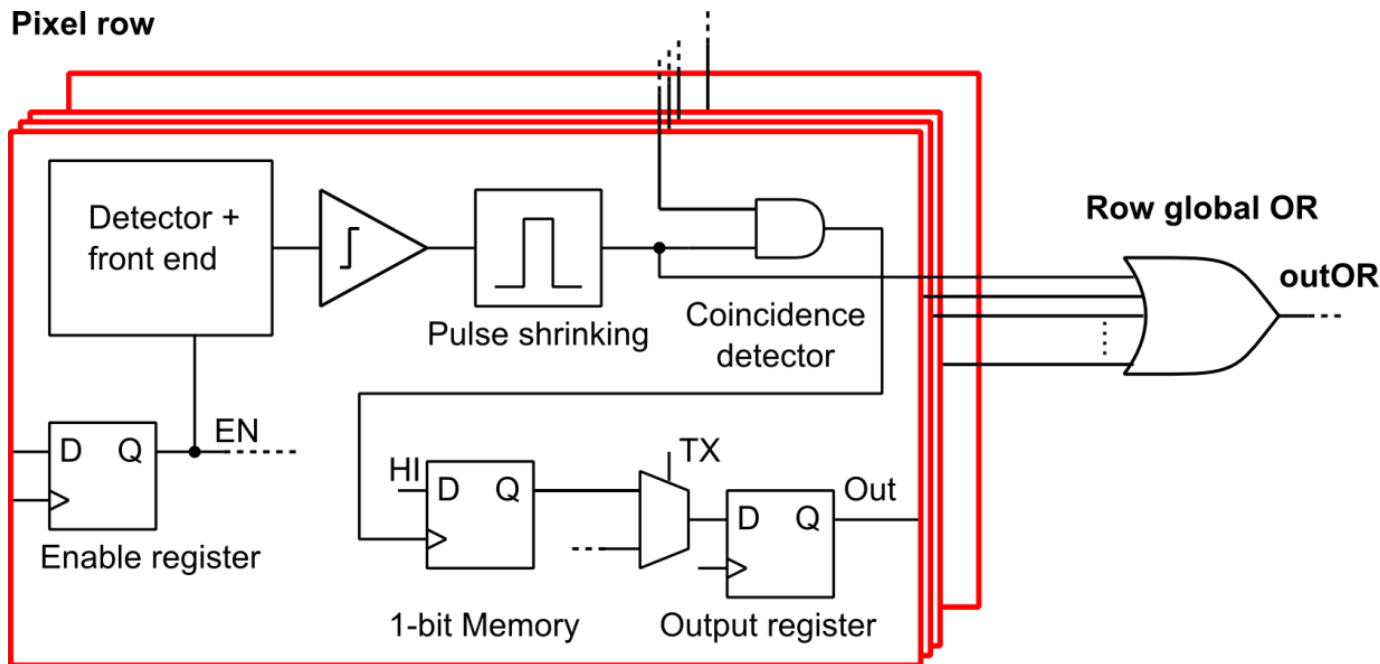
2-level pixel schematic

Top pixel: subset of bottom pixel

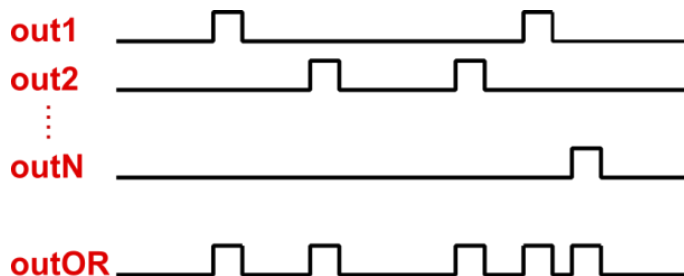




Sensor architecture: row-wise OR

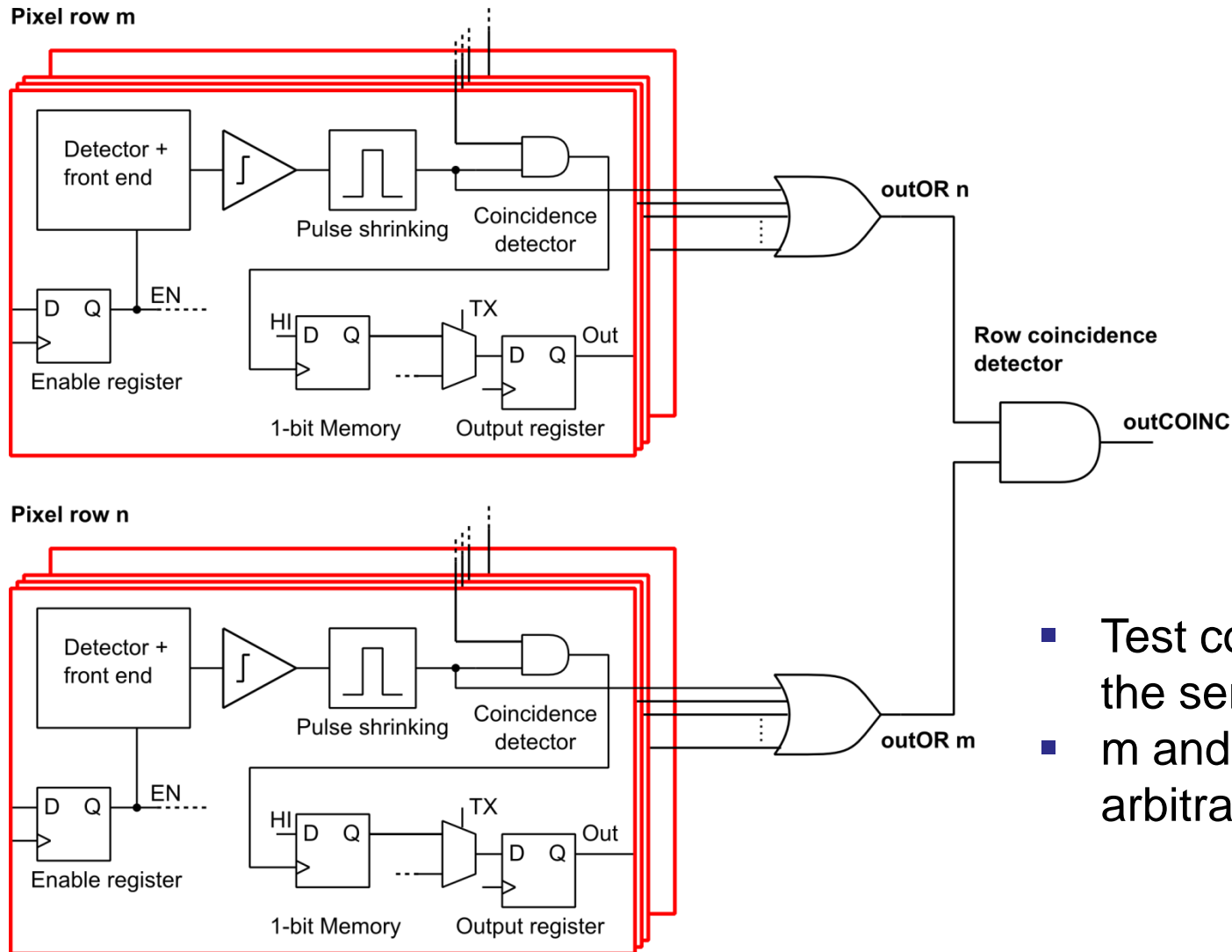


Test output outOR:
combination of all the active
(enabled) pixels in the row





Row-wise coincidence circuit

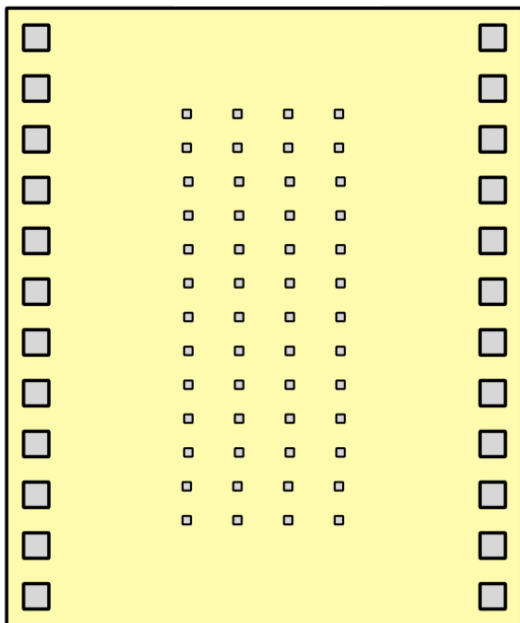


- Test coincidence in the sensor plane
- m and n can be arbitrarily selected

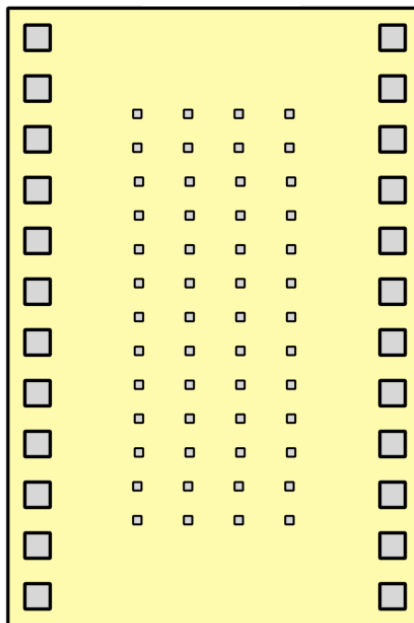


Sensor floorplan

Bottom chip



Top chip



- Pads for wire bonding
- Pads for bump bonding

Wire bonding pads on chip 2:
pre-integration test.

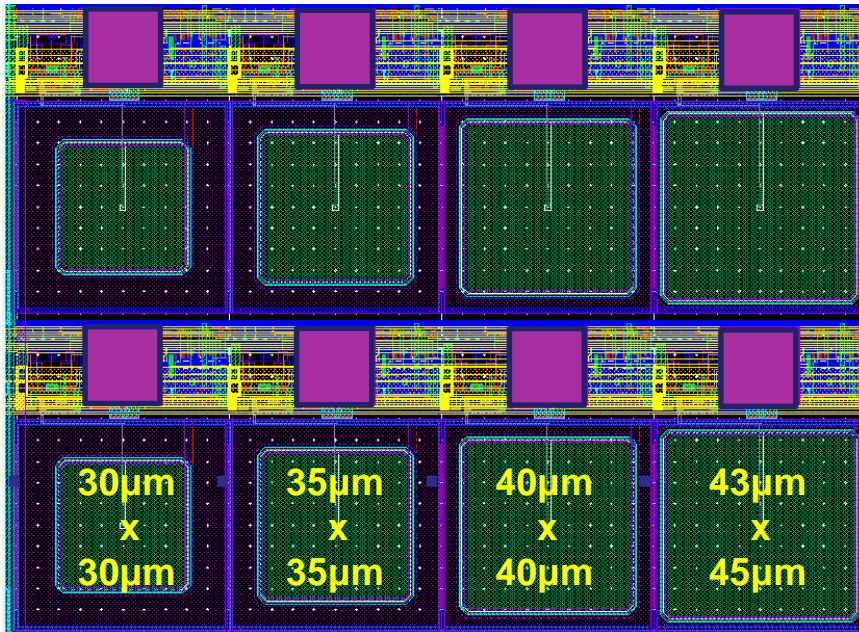


Final assembly

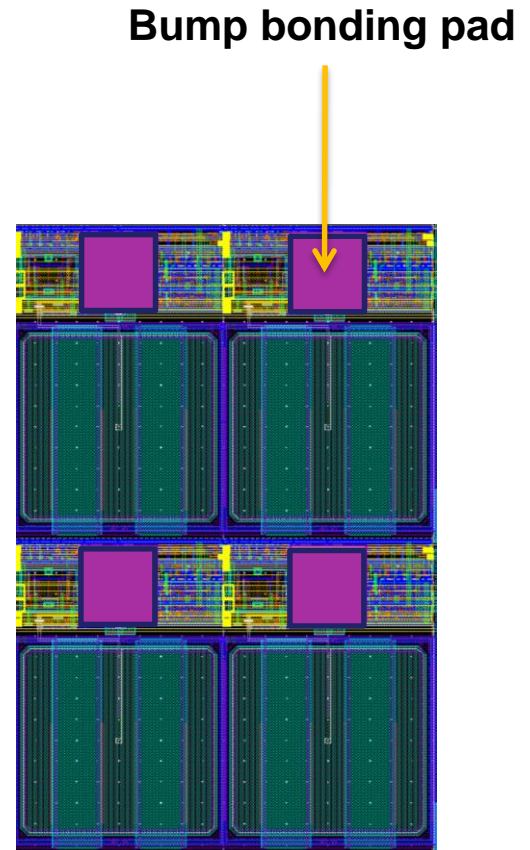


Pixel array

- 16 x 48 pixel array
- Pixel size: $50\mu\text{m} \times 75\mu\text{m}$
- Splittings in detector type and area



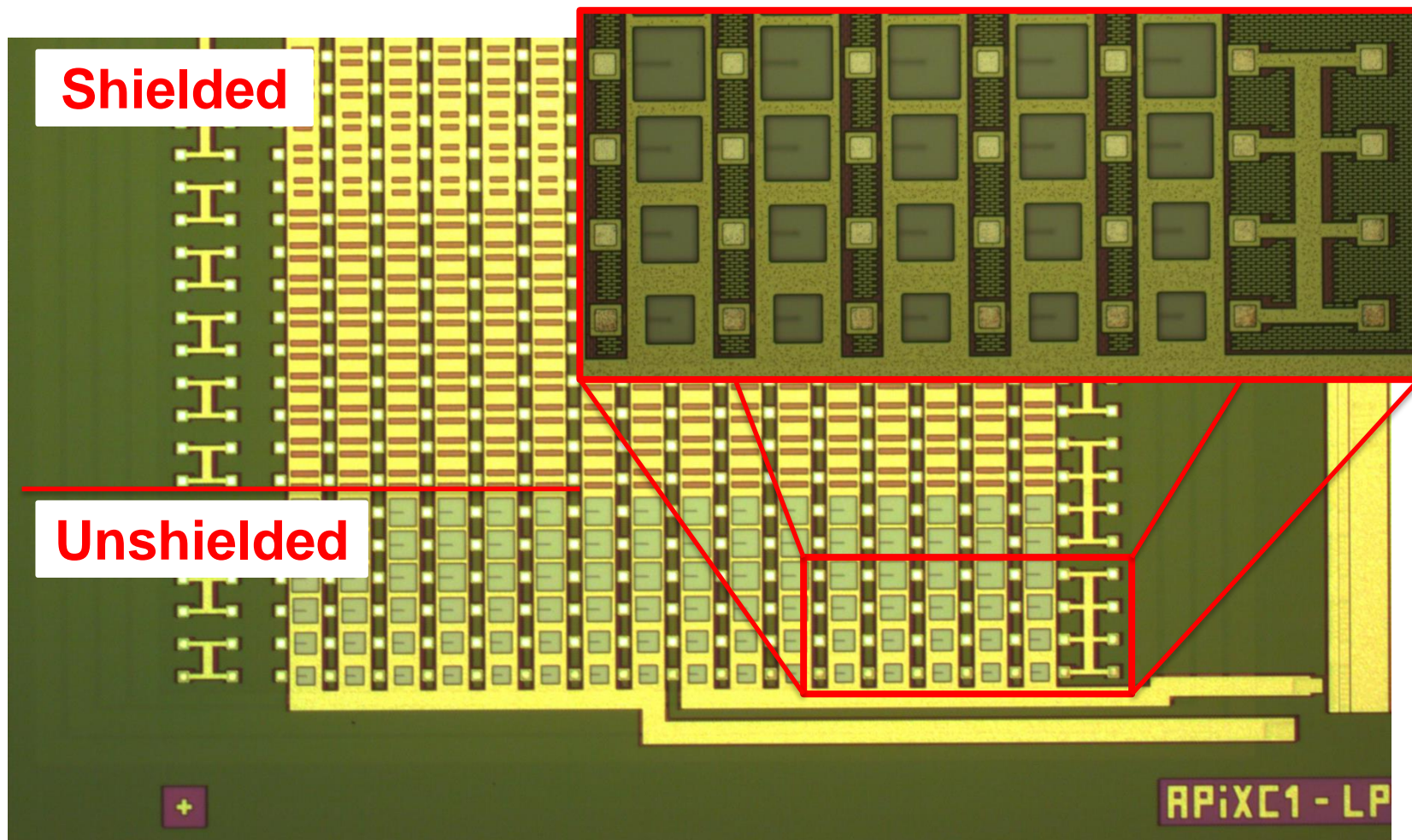
Pixels with different detector area
(unshielded)



Pixels with shielded
detectors



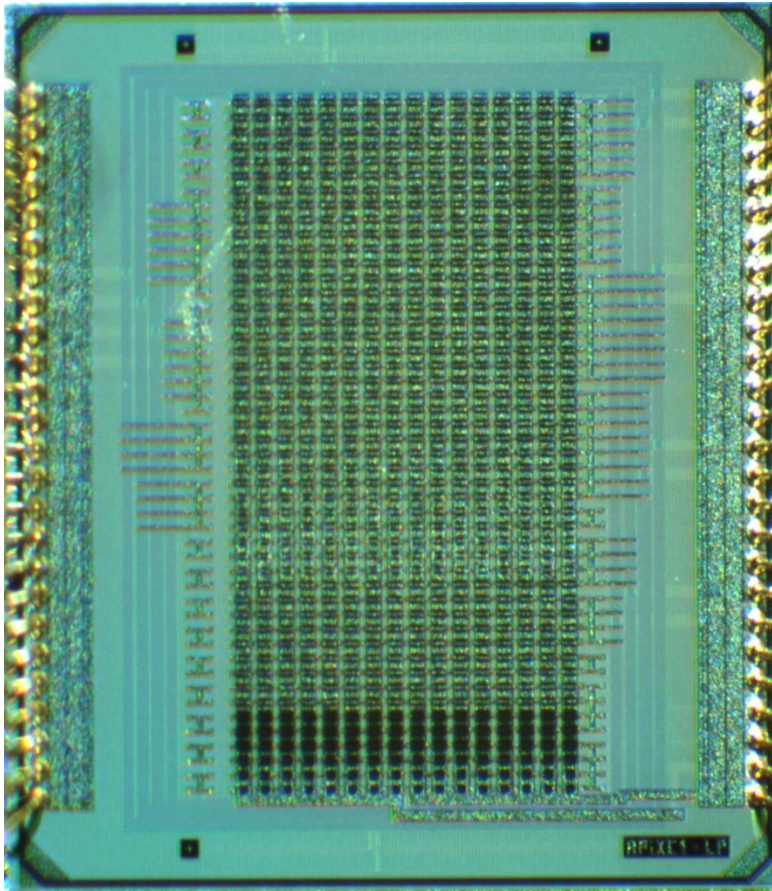
Bottom chip - Micrographs



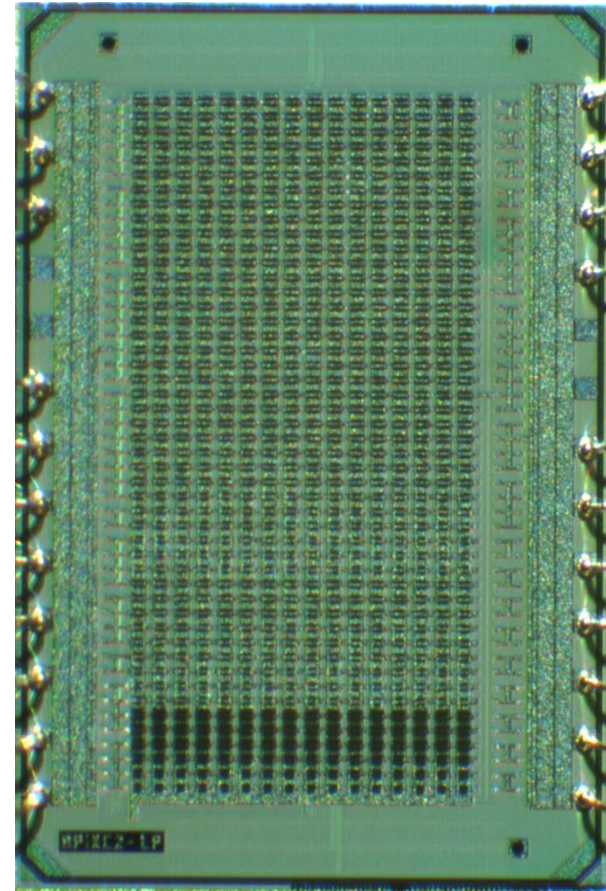


Sensor micrographs

Bottom chip



Top chip





Experimental results - summary

Characterization of **single-layer sensors**:

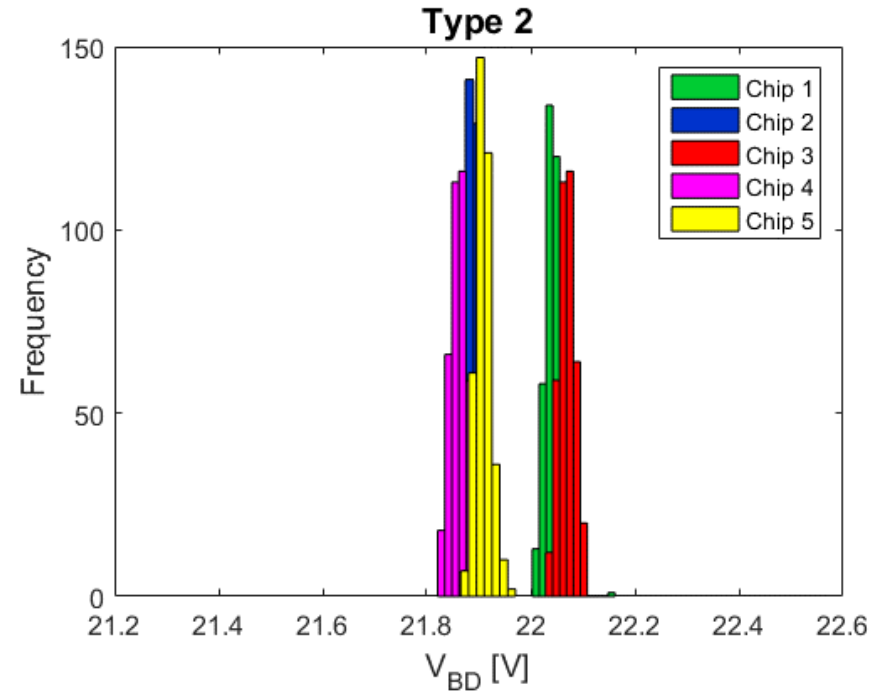
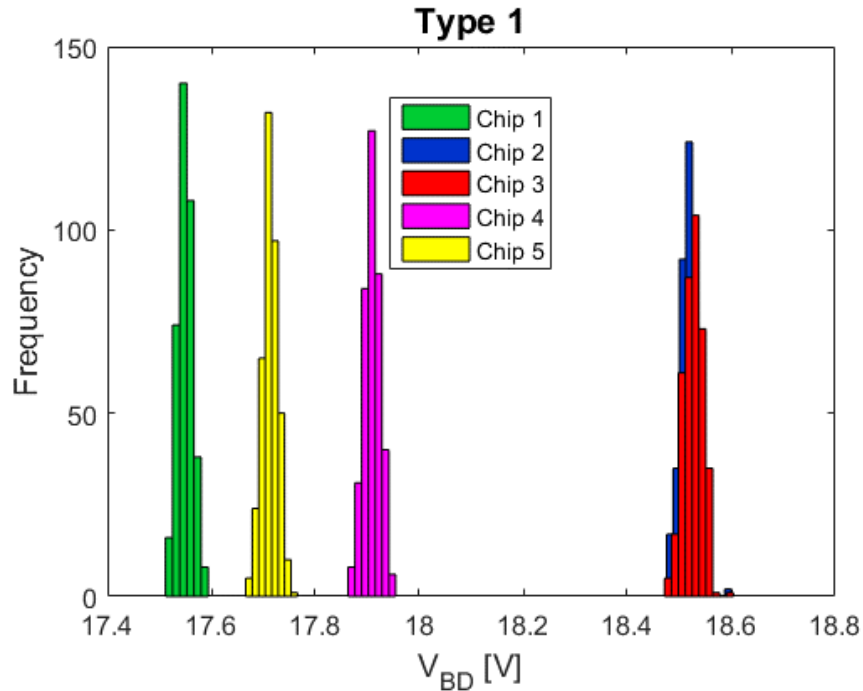
- **Core supply current (at 1.8V): 8mA**
- Breakdown voltage uniformity
- Dark count rate
- In-plane coincidence
- Timing resolution
- Cross-talk

Vertically integrated sensors with bump bonding (IZM):

- Coincidence dark counts
- Test with beta source
- Test beam



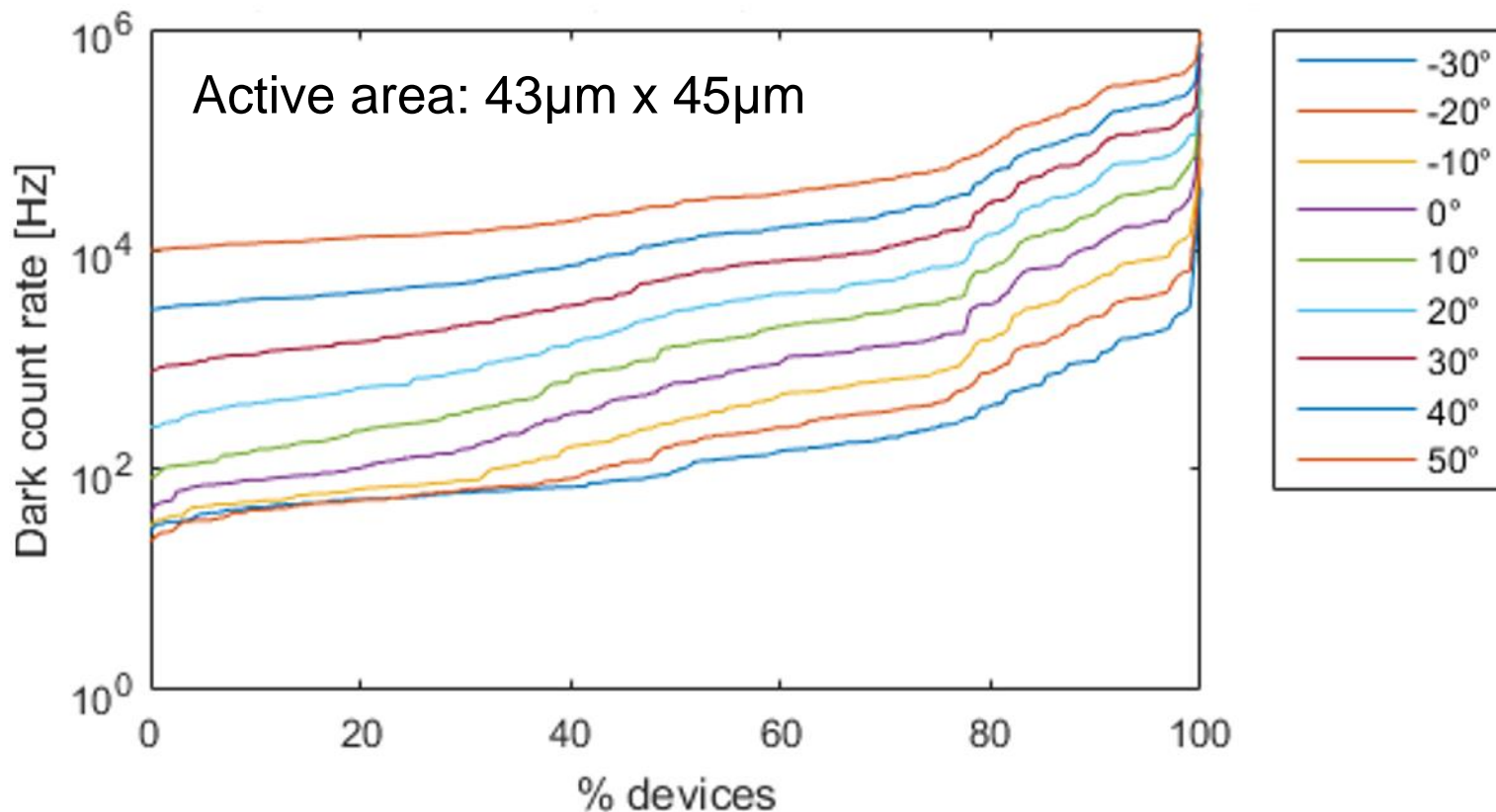
Breakdown voltage uniformity



- Measurements on
5 sample chips x 2 types x 196 devices per chip
- Very good uniformity on-chip ($\sigma < 20\text{mV}$)
- Large difference (1V) between different chips for type 1



DCR distribution

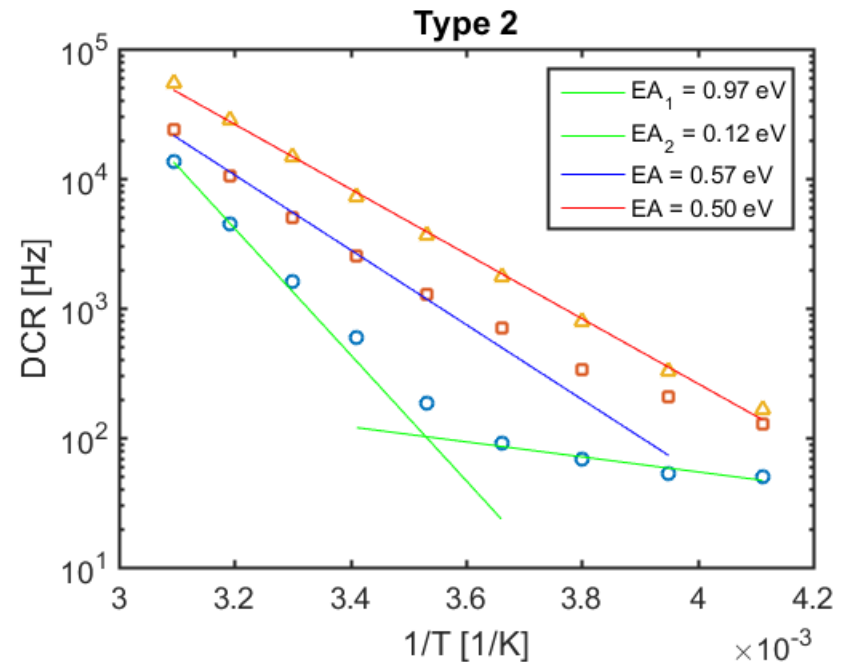
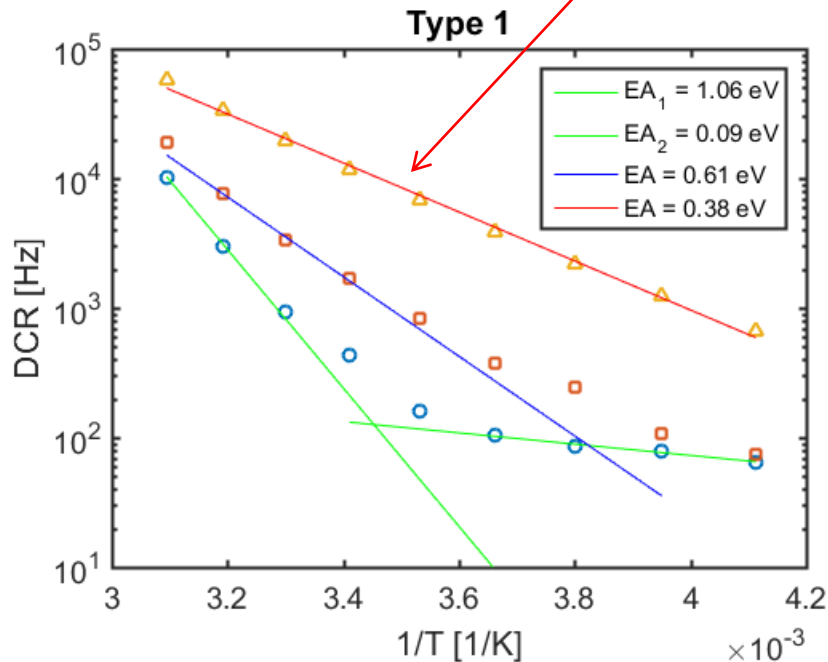


- DCR distribution spans 2 orders of magnitude at RT
- Median value at 20°C: 2.8kHz - MHz/mm²



DCR temperature dependence

Trap-assisted tunneling: $E_A < E_G/2$

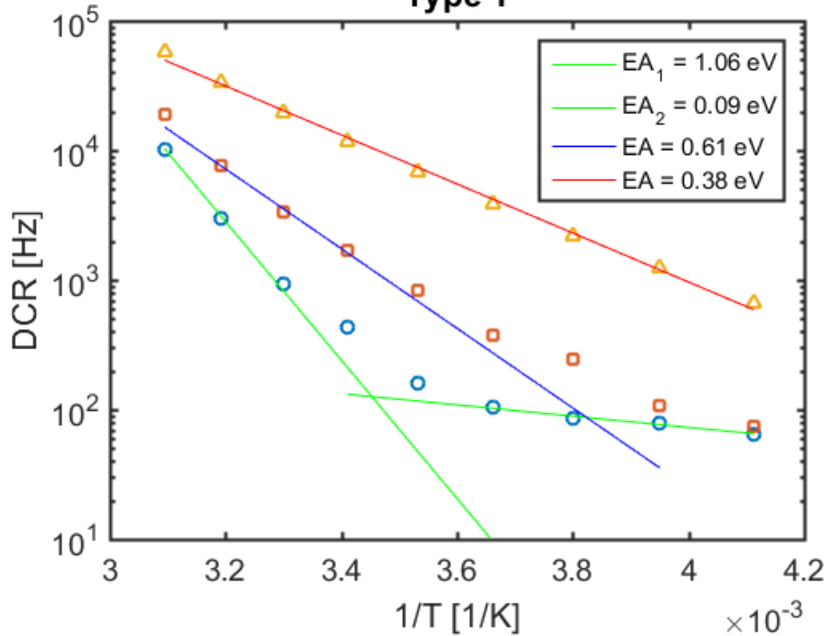


- Devices with $43\mu\text{m} \times 45\mu\text{m}$ active area, but different DCR
- Measurements from **-30°C to 50°C** with 10°C steps
- Overvoltage: $V_{OV} = 3.3\text{V}$



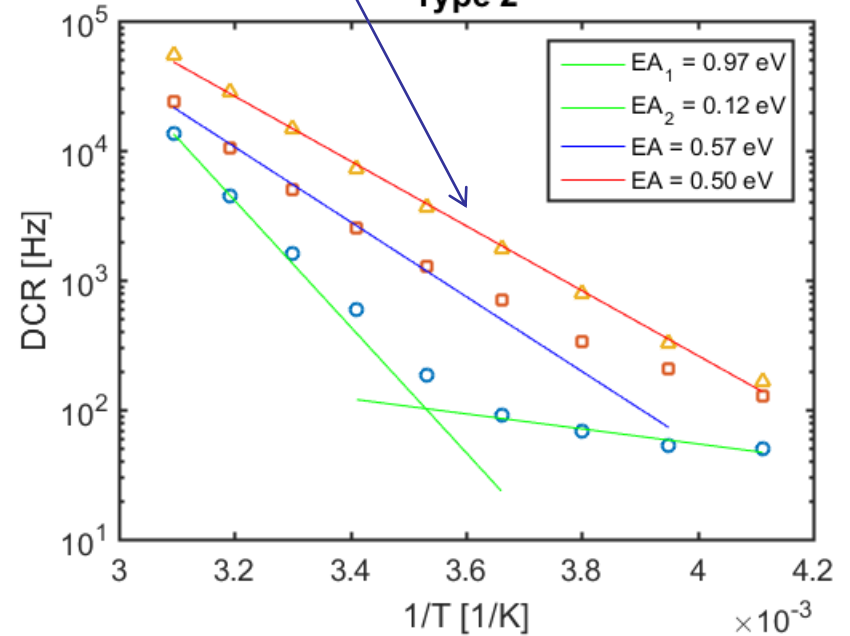
DCR temperature dependence

Type 1



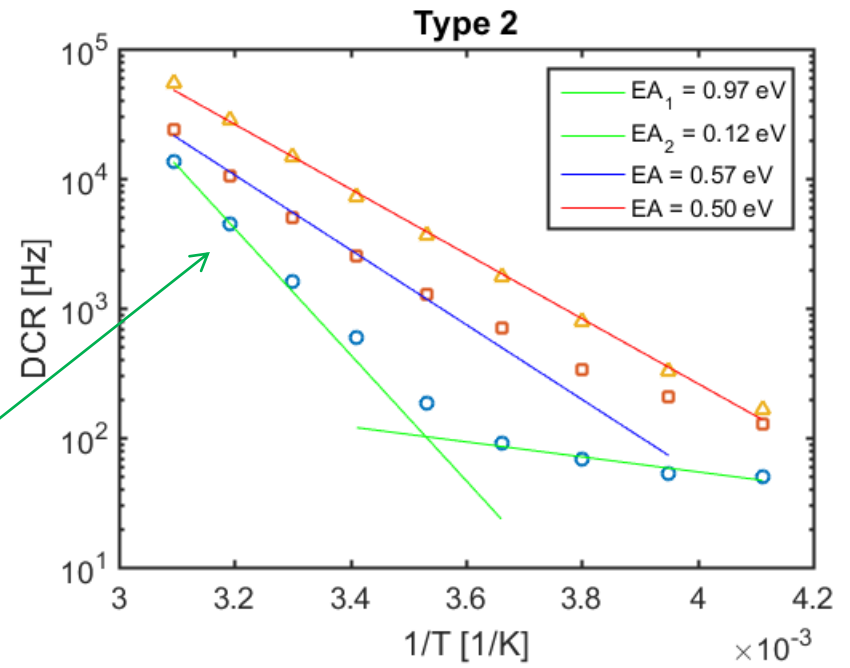
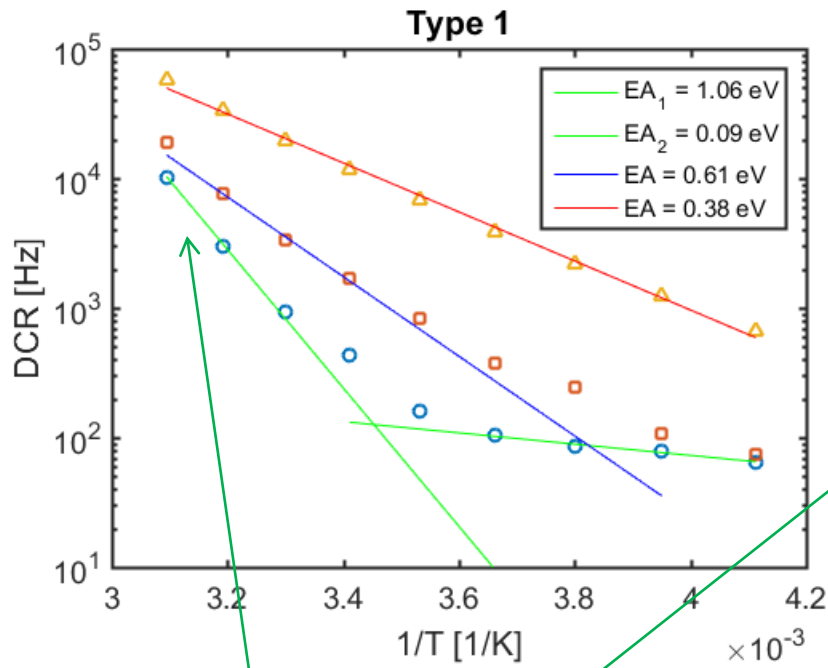
SRH generation $E_A \sim E_G/2$

Type 2





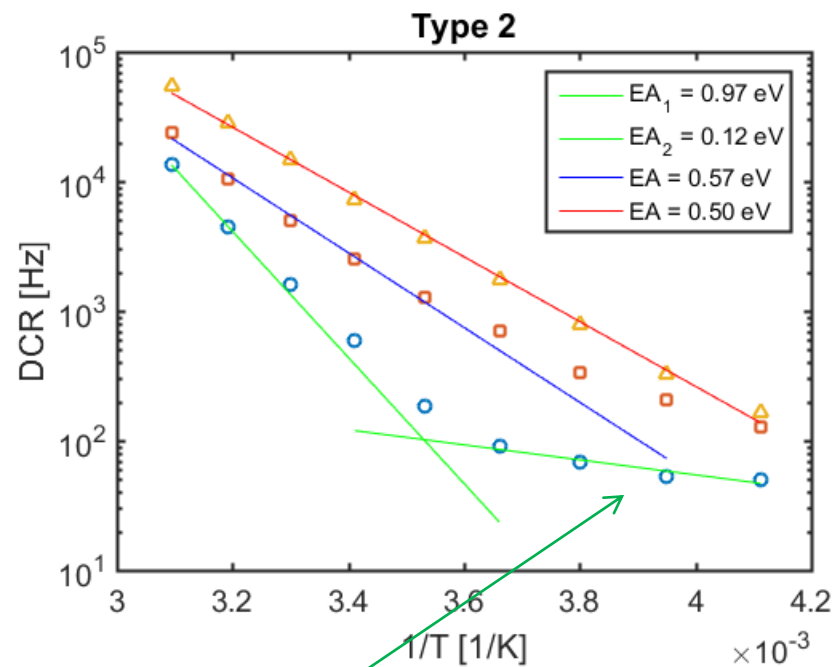
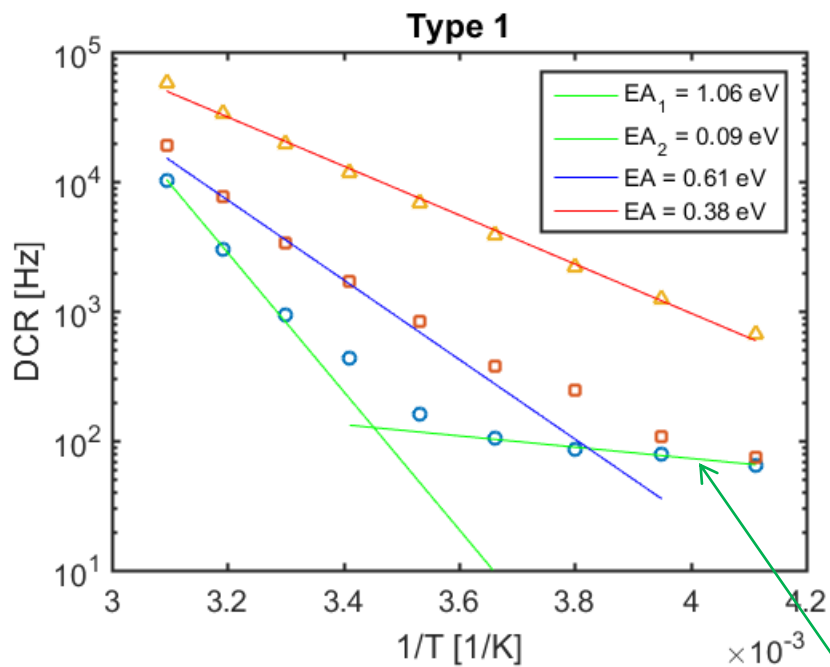
DCR temperature dependence



Injection from neutral regions: $E_A \sim E_G$



DCR temperature dependence



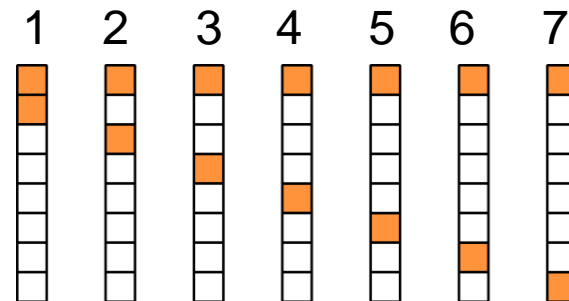
Band – to – band tunneling: $E_A \rightarrow 0$



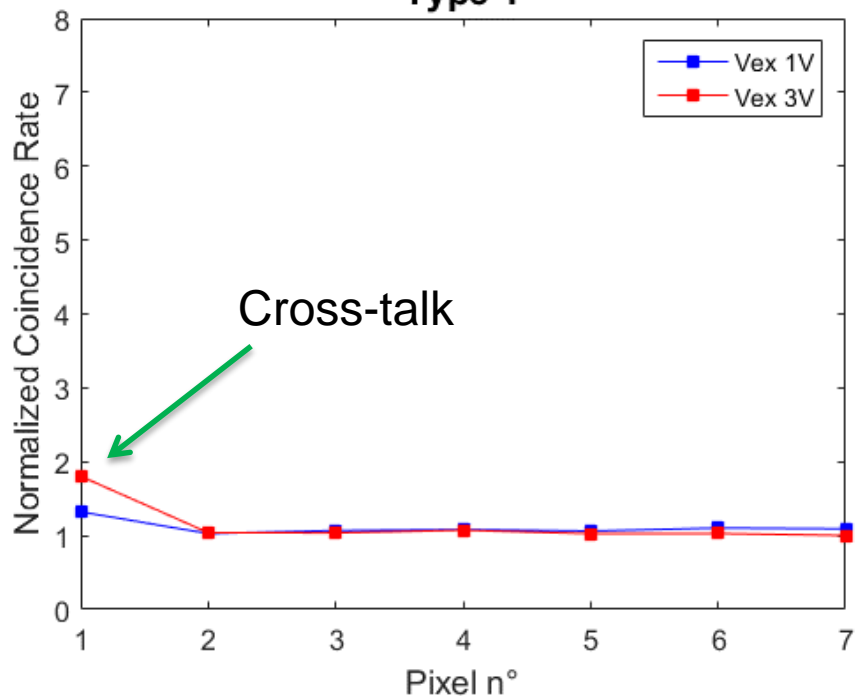
Coincidence detection

Count rate in coincidence between two pixels in the same column

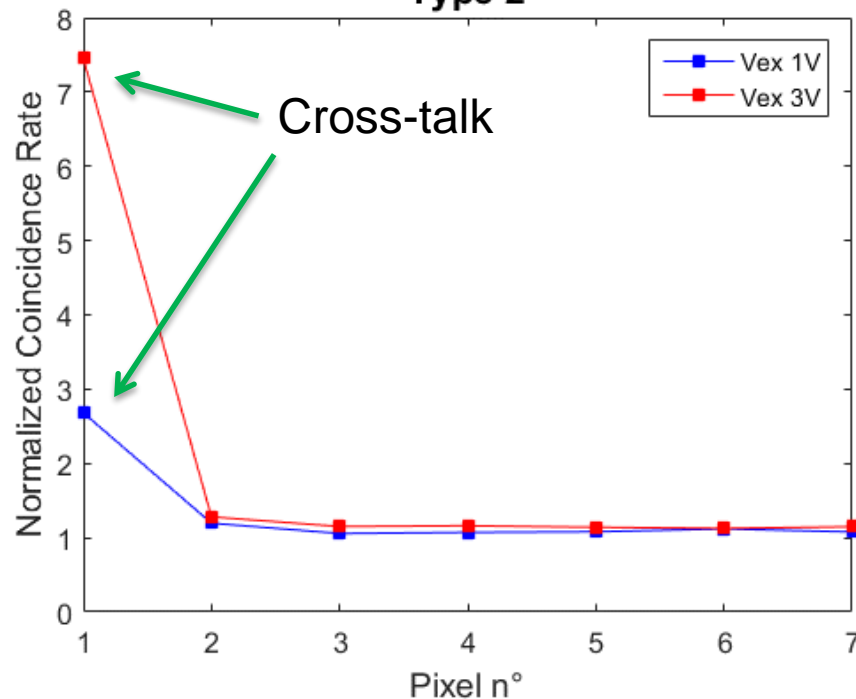
Normalized rate:
$$\frac{CR_{Meas}}{2 \cdot CR_1 \cdot CR_2 \cdot \Delta T}$$



Type 1



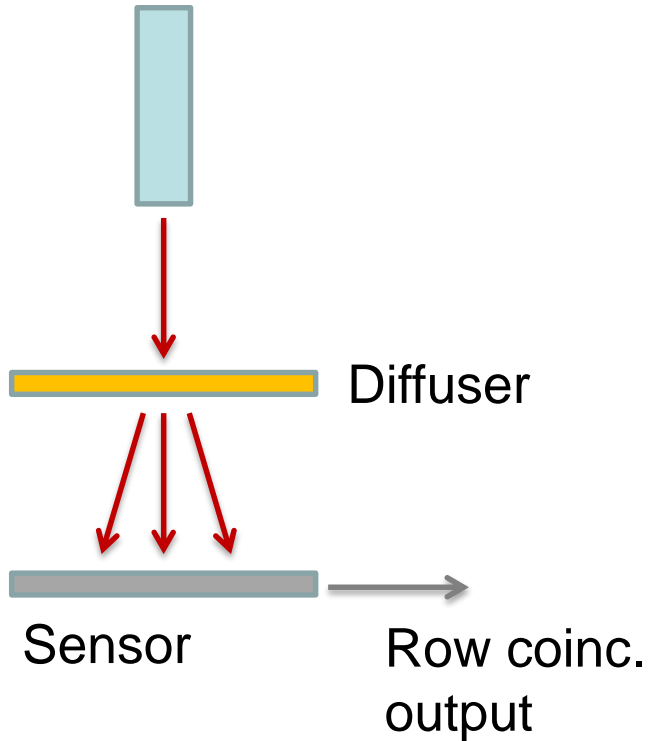
Type 2



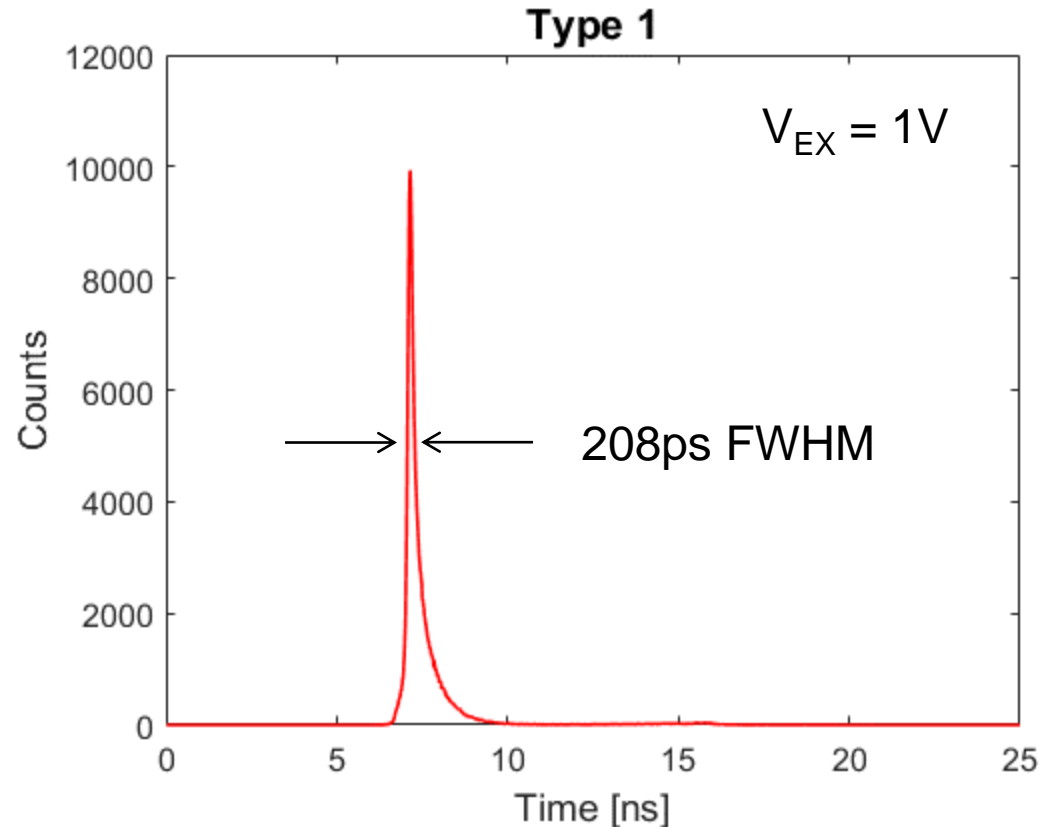


Timing resolution

IR laser (780nm)
50ps FWHM



2 pixels enabled

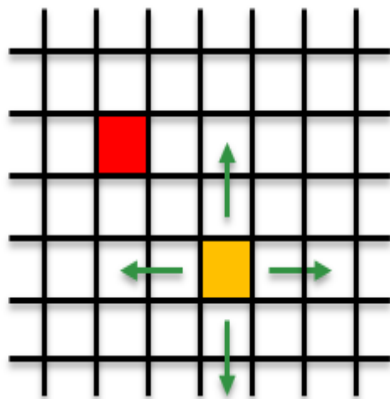


Timing histogram between laser trigger and sensor coincidence output

N.B. Design not optimized for timing



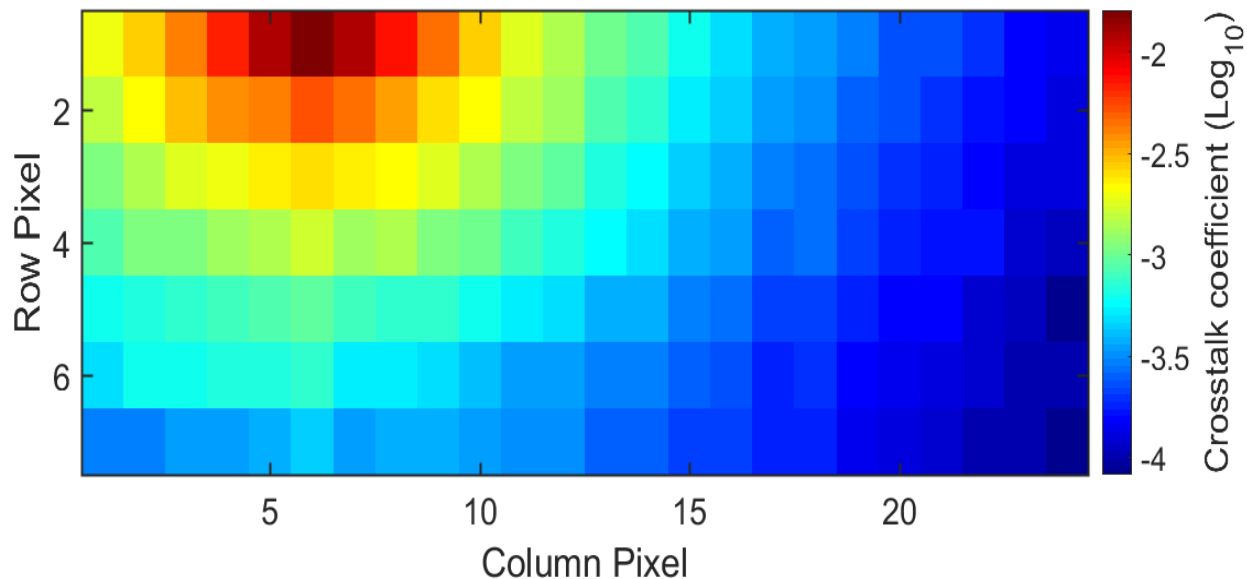
Crosstalk characterization



- **Emitter**
(fixed)
- **Detector**
(scan)

- Crosstalk coefficient

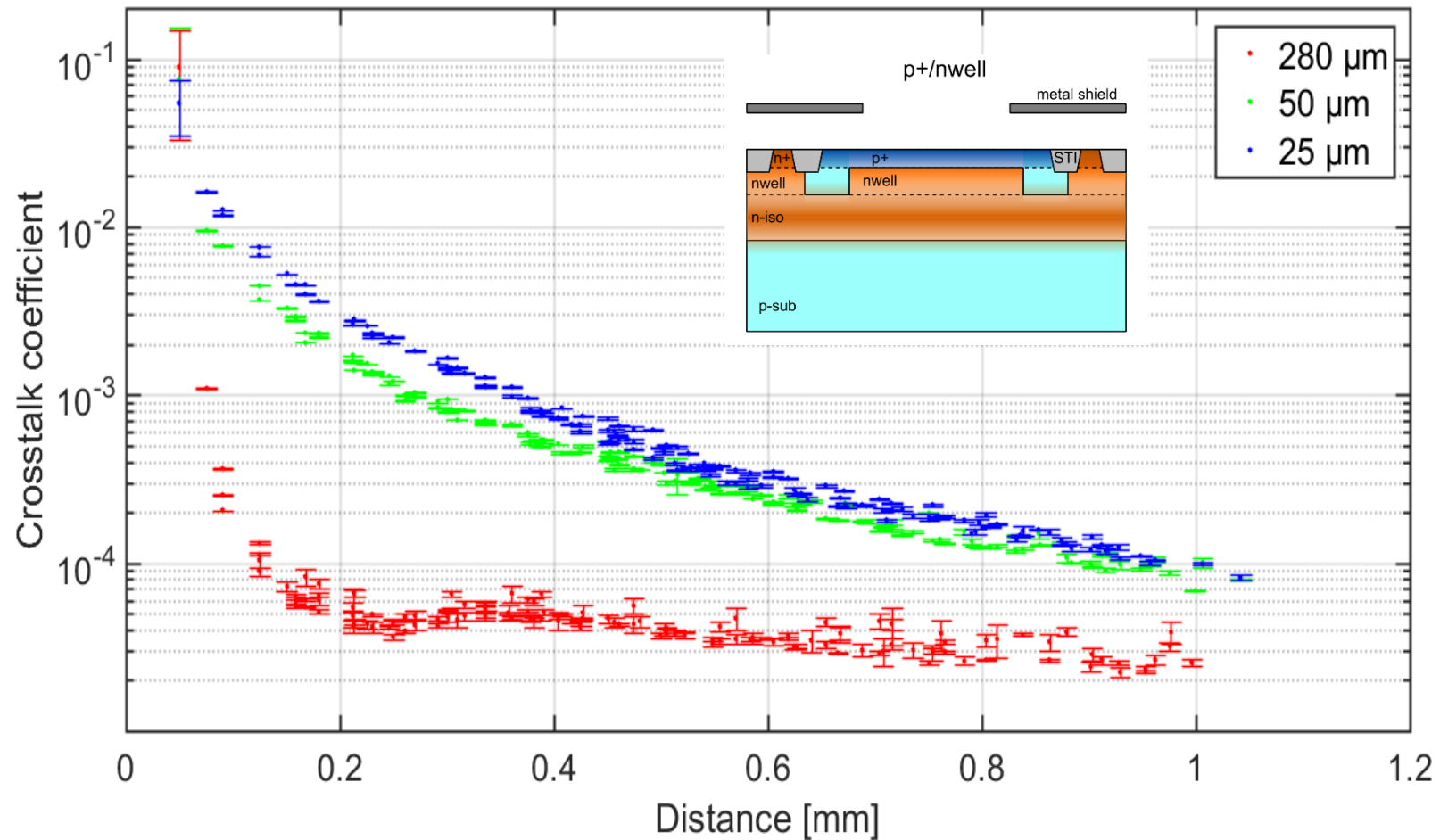
$$CR_m = DCR_e \cdot DCR_d \cdot 2\Delta T + K \cdot (DCR_e + DCR_d)$$



Crosstalk map – Type 1, 25 μ m thickness

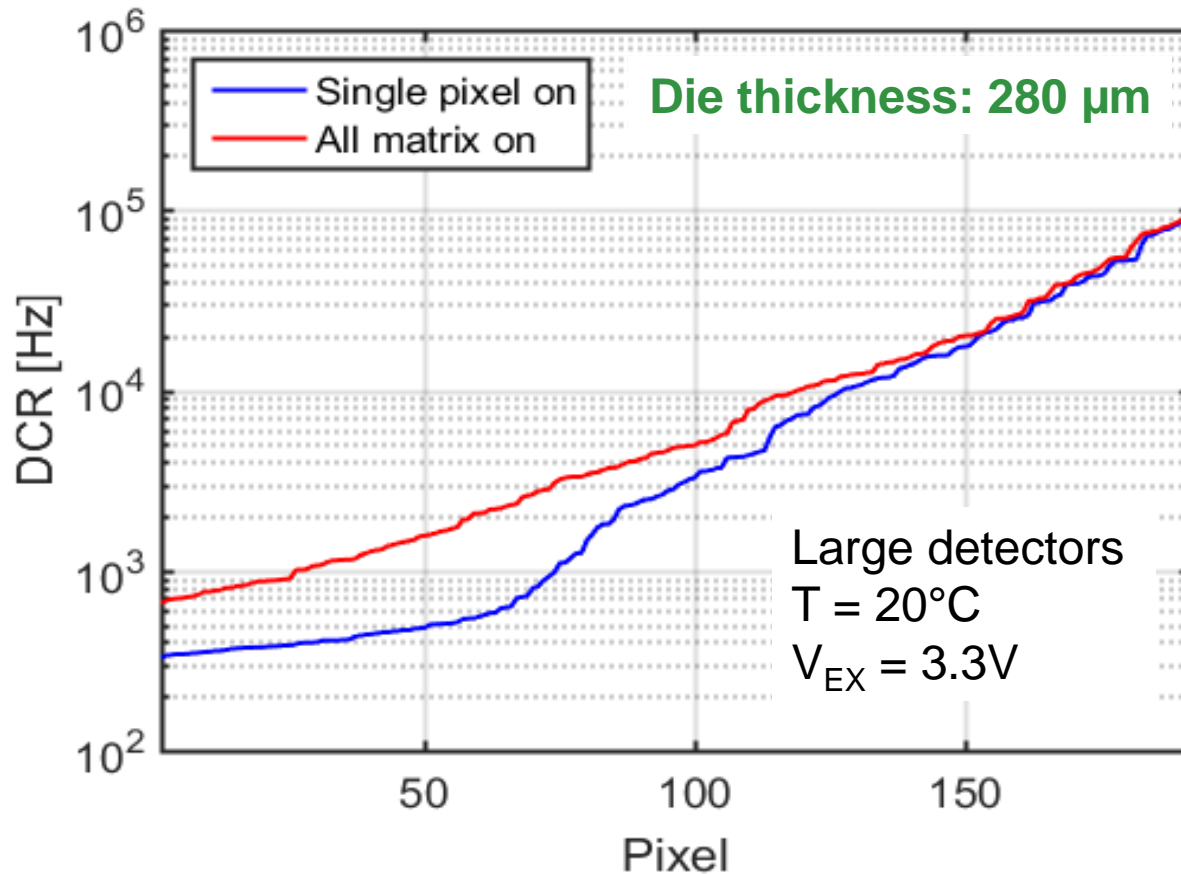


Crosstalk vs substrate thickness





Dark Count Rate and cross-talk



Median DCR increase of 70% due to cross-talk:
from 2.8kHz to 4.8kHz

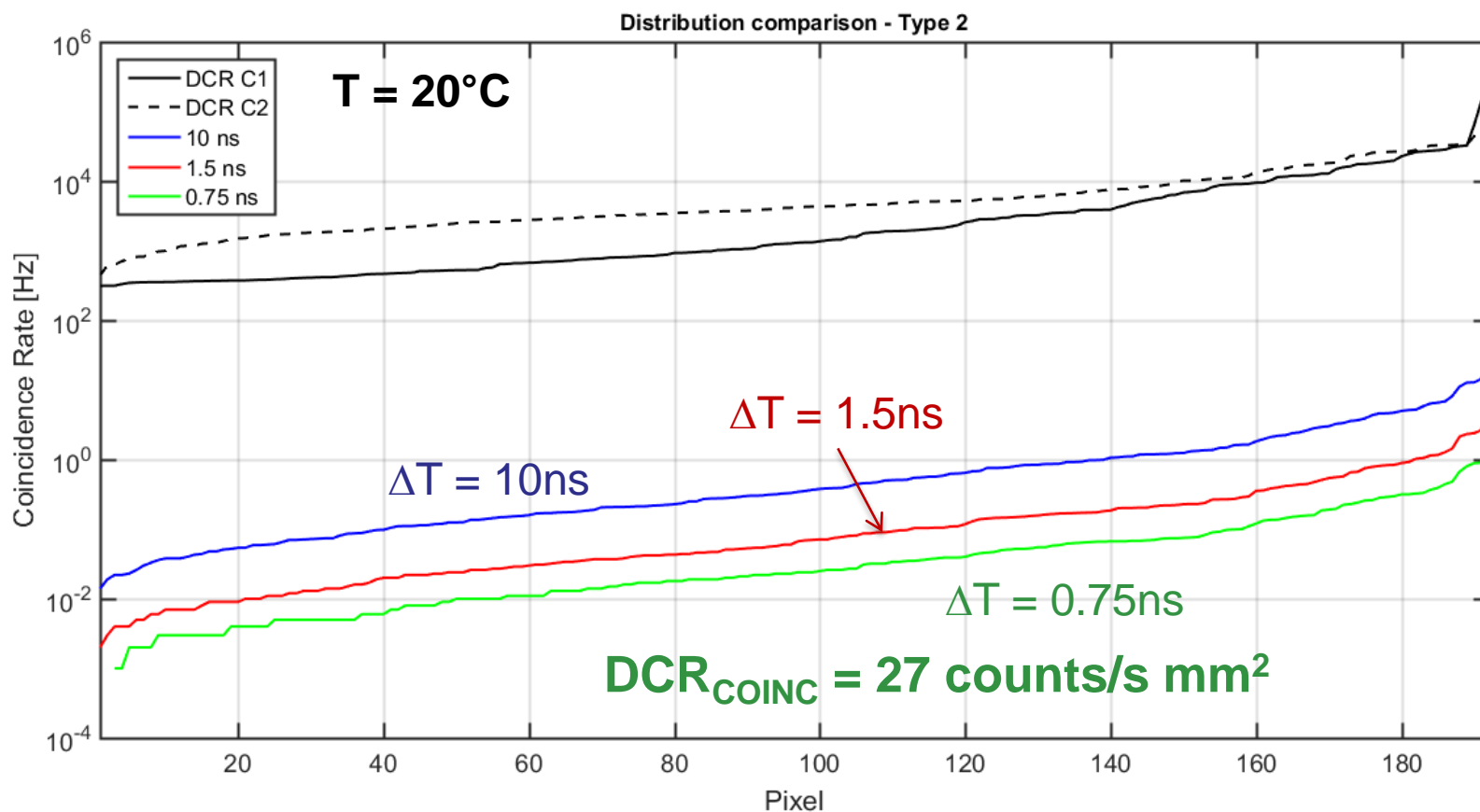
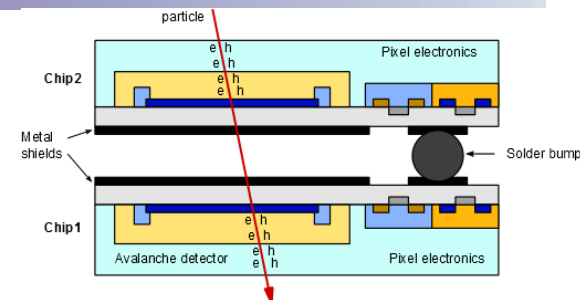
A. Ficorella, et a., Proc. IEEE ESSDERC, 2016



Vertically-integrated assembly

Dark Count Rate vs. coincidence time ΔT

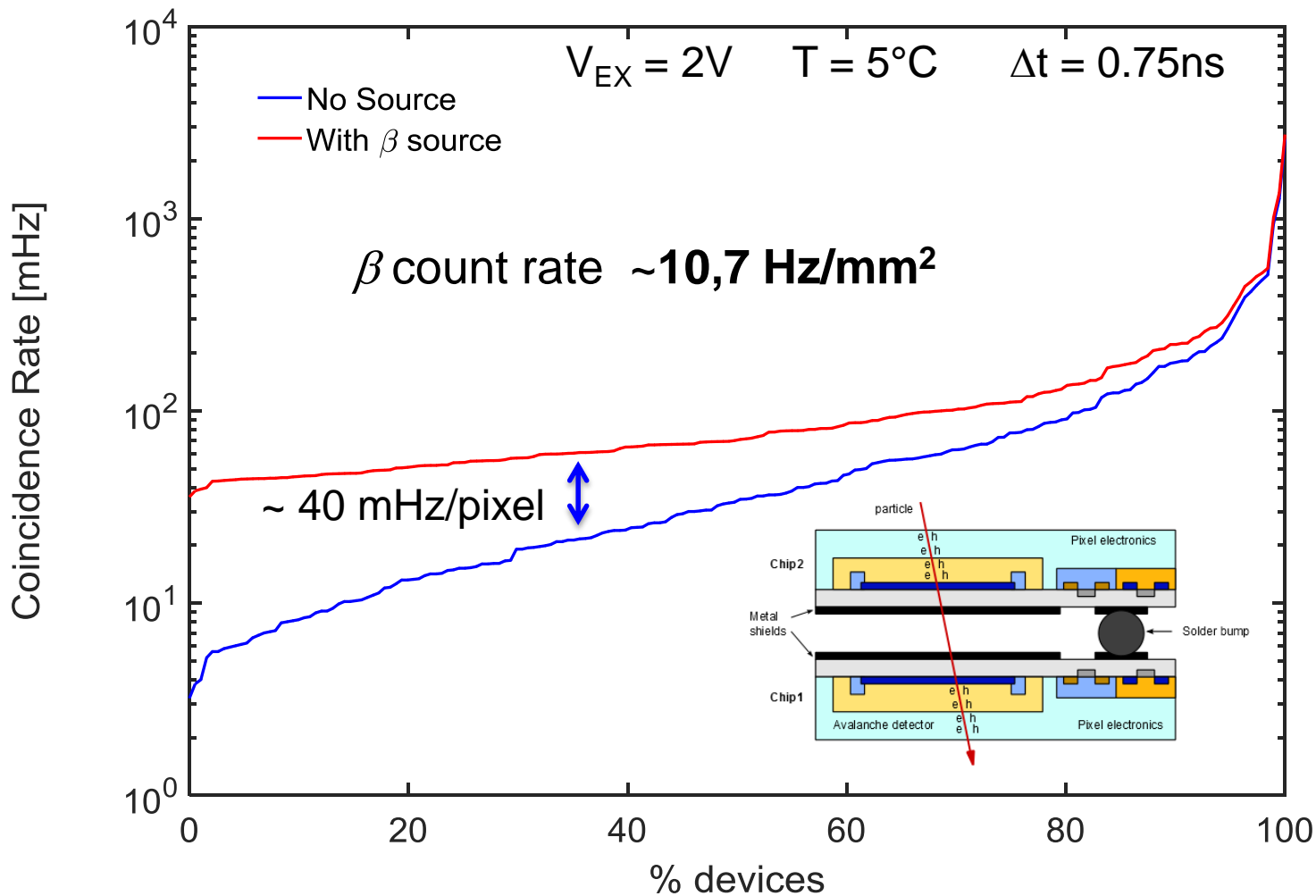
$$DCR_{COINC} = DCR_1 \times DCR_2 \times 2\Delta T$$





β -source measurements

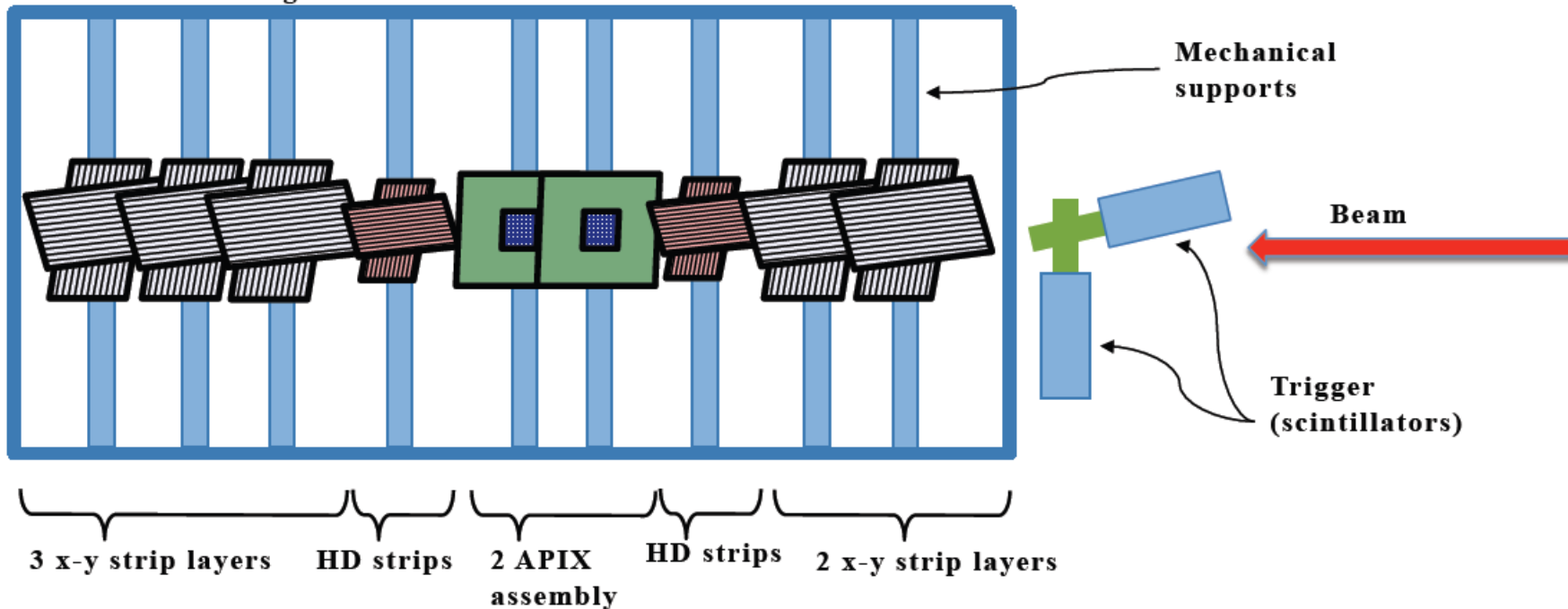
^{90}Sr β source – 37kBq at 2mm distance from sensor





Test beam at CERN

Metal box shielding

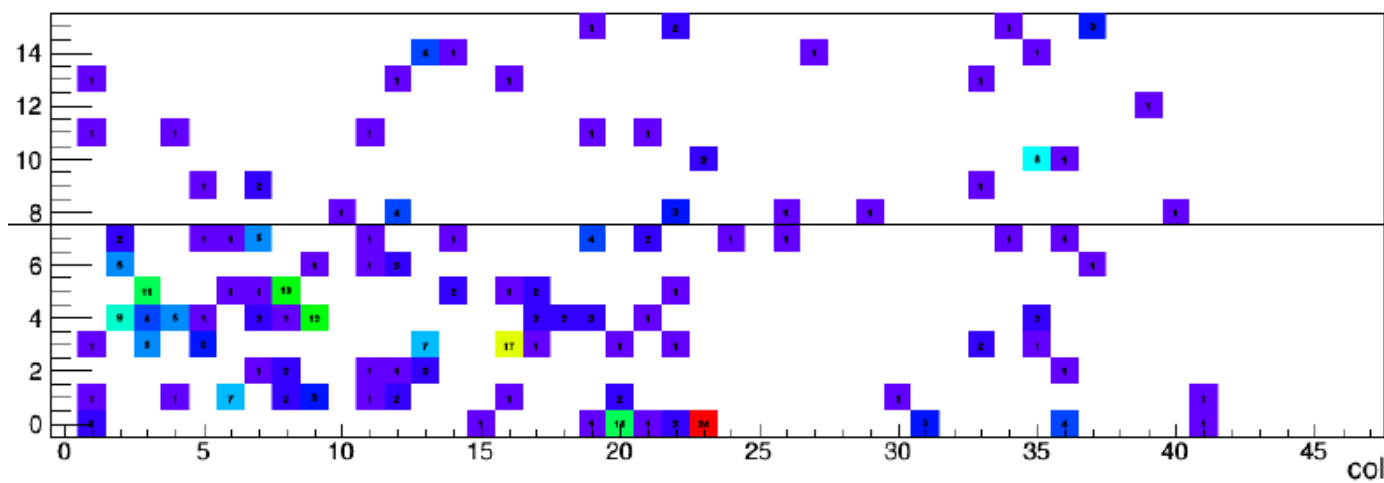


- Test at CERN SPS north area facility (H4 beam line)
- Two APIX under test + auxiliary Beam Tracker detector
- Positrons and π^+ beams at 50, 100, 150, 200 and 300 GeV

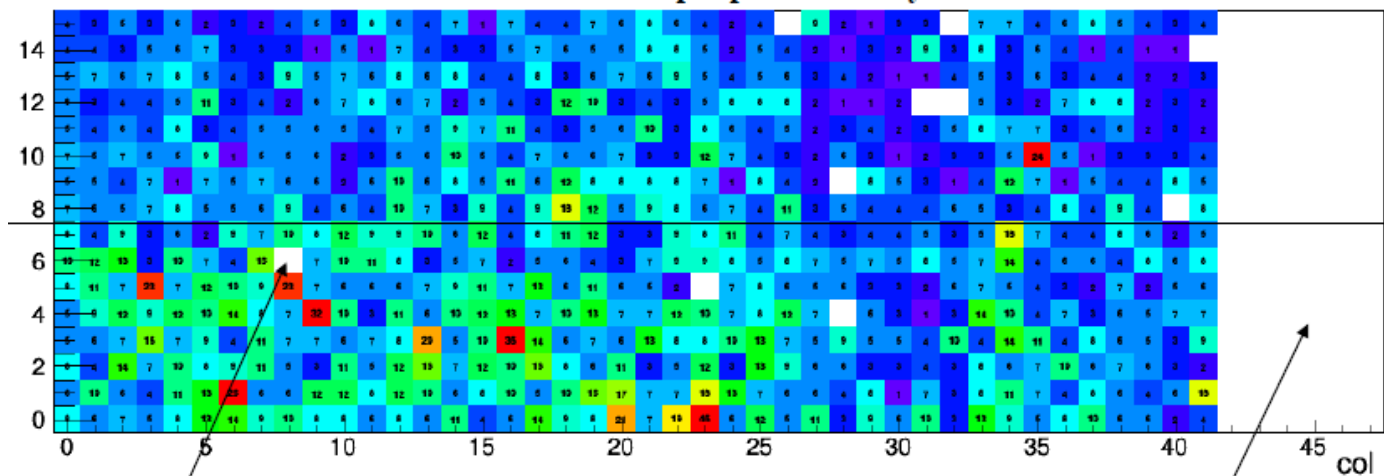


Test beam – hit maps

APIX random trigger upstream layer



APIX hitmap upstream layer



Noisy pixel disabled

Unshielded pixels disabled



APiX - Summary

Strengths:

- Can be thinned to a **few microns**: low material budget
- **Timing resolution**
- Low **power consumption**
- Early signal digitization

Weaknesses:

- Radiation tolerance (still to be assessed)
- Efficiency: guard ring and in-pixel electronics
- Cost and availability of 3D integration technologies



Current - future work

- Current prototype:
 - **Test beam** data analysis (in progress)
 - Radiation hardness studies
- Design of **new prototype**:
 - Improved fill factor
 - Larger array
 - Optimized timing
 - Optimized power consumption



Summary

- Highly parallel SPAD systems require high-density digital circuit for high efficiency
- SPAD technology in **deep sub-micron** processes is evolving driven by consumer applications: investments
- Maximum efficiency: **3D integration**. Optical cross-talk is still an issue in systems with very high FF
- Concept of charged-particles direct detection with Geiger-mode detectors in coincidence is feasible
- Efficiency is still an issue, but **timing** can be very good
- Development in deep-submicron SPADs and 3D integration can be the key for a full exploitation of this concept



Acknowledgements

APIX2 project

“Development of an Avalanche Pixel Sensor for tracking applications”

Funded by **INFN** – CSN5

Project coordinator: Pier Simone Marrocchesi, INFN Pisa and
University of Siena

Partners:

- TIFPA and University of Trento,
- INFN Pavia and University Pavia,
- INFN Padova and University of Padova,
- Laboratoire APC, Université Paris-Diderot/CNRS